

AD-A008 590

CORRELATION OF FATIGUE DATA FOR ALUMINUM AIRCRAFT  
WING AND TAIL STRUCTURES

R. Hangartner

National Aeronautical Establishment

Prepared for:

National Research Council of Canada

December 1974

DISTRIBUTED BY:

**NTIS**

National Technical Information Service  
U. S. DEPARTMENT OF COMMERCE



National Research  
Council Canada

Conseil national  
de recherches Canada

AD-A008590

# CORRELATION OF FATIGUE DATA FOR ALUMINUM AIRCRAFT WING AND TAIL STRUCTURES

BY

R. HANGARTNER

NATIONAL AERONAUTICAL ESTABLISHMENT

OTTAWA

DECEMBER 1974

Reproduced by  
NATIONAL TECHNICAL  
INFORMATION SERVICE  
US Department of Commerce  
Springfield, VA. 22151

DDC  
RECEIVED  
MAY 9 1975  
REGISTRY  
D

NRC NO. 14555

AERONAUTICAL  
REPORT

ISSN 0077-554

DISTRIBUTION STATEMENT A

LR-582

Approved for public release;  
Distribution Unlimited

CORRELATION OF FATIGUE DATA  
FOR ALUMINUM AIRCRAFT WING  
AND TAIL STRUCTURES

CORRELATION ENTRE LES DONNEES DE FATIGUE  
RELATIVES AUX STRUCTURES D'AILE ET D'EMPENNAGE D'AVION  
EN ALUMINIUM

by/par

R. HANGARTNER

DDC  
RECEIVED  
MAY 9 1975  
RECEIVED  
D

A.H. Hall, Head/Chef  
Structures and Materials Laboratory/  
Laboratoire des structures et matériaux

F.R. Thurston  
Director/Directeur

DISTRIBUTION STATEMENT A

Approved for public release;  
Distribution Unlimited

## SUMMARY

S-N curves are derived for aluminum wing and tail structures by fitting various regression models to 246 full-scale constant-amplitude fatigue test results from twelve types of aircraft structures. The derived curves were tested by comparing the predicted lives with actual test results of various aircraft structures fatigue tested to variable-amplitude loads spectra. More reliable predictions resulted from these derived S-N curves than from existing S-N curves.

## RESUME

Les courbes de fatigue relatives aux structures d'aile et d'empennage sont obtenues grâce à l'étude, au moyen de modèles basés sur la méthode de regression, des 246 résultats des essais de fatigue en vraie grandeur, et à amplitude constante, entrepris sur douze types de cellules d'avion. Les courbes obtenues ont été contrôlées en comparant les durées de vie prévues aux résultats des essais de fatigue réels effectués, suivant un spectre de charges d'amplitude variable, sur différentes cellules d'avion. Ces nouvelles courbes permettent des prédictions plus fiables qu'avec les courbes de fatigue existantes.

## TABLE OF CONTENTS

	Page
SUMMARY .....	(iii)
TABLES .....	(v)
ILLUSTRATIONS .....	(v)
APPENDICES .....	(vi)
ABBREVIATIONS .....	(vi)
NOMENCLATURE .....	(vi)
1.0 INTRODUCTION .....	1
2.0 S-N CURVES DERIVED FROM FULL-SCALE STRUCTURES .....	1
3.0 CONSTANT-AMPLITUDE FATIGUE TEST RESULTS .....	2
3.1 Definitions, Assumptions and Other Relevant Information .....	2
3.2 General Comments on Fatigue Tests .....	3
4.0 ANALYSIS OF RESULTS .....	3
4.1 Mathematical Models .....	3
4.1.1 Log N Versus Log $S_a$ Curves .....	3
4.1.2 Log N Versus $S_a$ Curves .....	4
4.2 Residuals .....	5
5.0 COMPARISON OF S-N CURVES .....	5
6.0 SCATTER IN CONSTANT-AMPLITUDE FATIGUE DATA .....	6
6.1 Scatter Within a Group of Similar Structures .....	6
6.2 Scatter Due to Different Types of Structures .....	6
7.0 LIFE PREDICTIONS USING VARIOUS S-N CURVES AND RELIABILITY OF PREDICTIONS .....	7
7.1 Lives Predicted by Various S-N Curves .....	7
7.2 Reliability of Predictions .....	8
8.0 CONCLUSIONS .....	9
9.0 REFERENCES .....	9

### TABLES

Table		Page
1	Constant-Amplitude Data Used in Analysis .....	13
2	Results of Various Regressions .....	14
3	Variable-Amplitude Tests .....	15
4	Life Predictions Resulting from the Use of Various S-N Curves Compared with Log-Means of Actual Tests. Al-Cu-Mg Alloy Structures .....	16
5	Life Predictions Resulting from the Use of Various S-N Curves Compared with Log-Means of Actual Tests. Al-Zn-Mg Alloy Structures .....	17
6	Summary of Damage Ratios of Life Predictions Using Various S-N Curves .....	18

### ILLUSTRATIONS

Figure		Page
1	Experimental Data .....	19
2	Average Endurances of Complete Wings and Tailplanes .....	20
3	Coefficients of Equations Representing RAeS S-N Curves vs Mean Stress .....	21
4	Experimental Data, Al-Cu-Mg Alloys .....	22
5	Experimental Data, Al-Zn-Mg Alloys .....	23
6	S-N Curve No. 1, Al-Cu-Mg Alloy Structures, Linear S-N Curve .....	24
7	S-N Curve No. 1, Al-Zn-Mg Alloy Structures, Linear S-N Curve .....	25
8	S-N Curve No. 2, Al-Cu-Mg Alloy Structures, Quadratic S-N Curve .....	26
9	S-N Curve No. 2, Al-Zn-Mg Alloy Structures, Quadratic S-N Curve .....	27
10	S-N Curve No. 3, Al-Cu-Mg Alloy Structures, Quadratic S-N Curve .....	28
11	S-N Curve No. 3, Al-Zn-Mg Alloy Structures, Quadratic S-N Curve .....	29
12	S-N Curve No. 4, Al-Cu-Mg Alloy Structures, Cubic S-N Curve .....	30
13	S-N Curve No. 4, Al-Zn-Mg Alloy Structures, Cubic S-N Curve .....	31
14	Residuals vs Estimated Life for S-N Curve No. 1 (All Alloys) .....	32
15	Comparison of RAeS S-N Curves and S-N Curve No. 1 (Al-Cu-Mg) .....	33

### ILLUSTRATIONS (Cont'd)

Figure		Page
16	Actual vs Predicted Lives for S-N Curve No. 1 (All Alloys) .....	34
17	Probability of Damage Ratios Being Exceeded for S-N Curve No. 1 and RAeS S-N Curves .....	35
18	Probability of Damage Ratios Being Exceeded for S-N Curve No. 2 and RAeS S-N Curves .....	36
19	Probability of Damage Ratios Being Exceeded for S-N Curve No. 3 and RAeS S-N Curves .....	37
20	Probability of Damage Ratios Being Exceeded for S-N Curve No. 4 and RAeS S-N Curves .....	38
21	Comparison of $\sum \frac{n}{N}$ Values for Various S-N Curves at Equal Reliabilities .....	39

### APPENDICES

Appendix		Page
I	Methods for Interpolating Between the RAeS S-N Curves .....	41
II	Computer Output of Typical Life Calculation .....	43

### ABBREVIATIONS

ESDU	Engineering Sciences Data Unit
ksi	kips per square inch
RAeS	Royal Aeronautical Society

### NOMENCLATURE

A, B, C, D	coefficients
$b_1, b_2, \dots b_i$	coefficients
$f, f_1, \dots f_i$	general functions
M	material parameter in regression equation
n, N	number of cycles

### NOMENCLATURE (Cont'd)

$S_a, S_{alt}$  alternating stress (ksi)

$S_m, S_{mean}$  mean stress (ksi)

$\sigma$  standard deviation

## CORRELATION OF FATIGUE DATA FOR ALUMINUM AIRCRAFT WING AND TAIL STRUCTURES\*

### 1.0 INTRODUCTION

This document establishes more consistent S-N curves for the fatigue life prediction of aluminum aircraft wing structures than the presently available RAeS-ESDU S-N curves for "Typical Wings and Tailplanes" (Ref. 1).

Constant-amplitude fatigue test results from 246 aircraft wings and tails from twelve aircraft types were pooled and various regression models were fitted in order to obtain mathematical expressions for sets of S-N curves.

These curves and the existing RAeS-ESDU curves were then used to predict the lives of variable-amplitude tests and the calculated lives were compared with the actual test results.

In the life calculations the method of linear cumulative damage (Palmgren-Miner Rule) was utilized.

### 2.0 S-N CURVES DERIVED FROM FULL-SCALE STRUCTURES

When estimating the life of a wing structure when structural details and an extensive stress analysis of the wing are not available it is normally better to use S-N curves derived from built-up structures than those derived from notched material coupons. Reasons for this include the fact that there is no fretting in a simple specimen and a simple specimen has only one load path whereas many structures are redundant.

RAeS-ESDU published a set of S-N curves derived from 137 full-scale fatigue tests on wings and tailplanes of various aluminum alloy aircraft structures (Ref. 1). These data and curves are reproduced in Figures 1 and 2.

Upon inspection of Figure 2 it is noticed that the curves do not follow the same general trend. It is easily seen that the line for five ksi mean stress does not follow the pattern of the lines for the other mean stresses. It is understood that the curves were drawn by "eye" and to illustrate this inconsistency the slopes and intercepts of the lines were plotted.

Straight lines on log-log plots can be expressed by the equations

$$\log_{10} N = A + B \log_{10} S_a$$

or

$$\log_{10} S_a = C + D \log_{10} N$$

The coefficients A, B, C and D were calculated for the lines shown in Figure 2 and their values were plotted versus mean stress in the graphs shown in Figure 3. The discontinuities in the curves tend to confirm that a mathematical analysis was not performed on the data.

Because of this and together with the fact that many additional data are now available it was decided to re-analyze the data and to include as many new data as could be obtained.

---

\* The work in this report is a summary of the author's Master's Thesis submitted at the University of Waterloo, Waterloo, Ontario, Canada.

### 3.0 CONSTANT-AMPLITUDE FATIGUE TEST RESULTS

In a literature search approximately 400 full-scale test results were located; however, only 246 were used in the analysis. The criteria for data selection were as follows:

- 1) The nominal stresses in the failure regions were well defined.
- 2) Only data from constant-amplitude tests were used in the analysis.
- 3) All data used had fatigue lives in the range  $10^3 \leq N \leq 10^7$  cycles.
- 4) All data used were from tests conducted at room temperature.

Table 1 lists the types of structures, the number of results used, and the references from which they were obtained. Reference 16 gives a more detailed list of the test results used in the analysis. The test results are plotted in Figures 4 and 5, these figures showing the test results for the Al-Cu-Mg alloys (e.g. 2024, and similar alloys) and the Al-Zn-Mg alloys (e.g. 7075) respectively.

#### 3.1 Definitions, Assumptions, and Other Relevant Information

1. Approximately three-quarters of the structures were manufactured from Al-Cu-Mg alloys and one-quarter of the structures from Al-Zn-Mg alloys. Preliminary analysis showed that a large difference in fatigue life existed between these two types of structures; thus, allowance had to be made for this in the analysis.
2. Failure was defined as final or catastrophic failure, i.e. the applied load could no longer be supported by the structure. An analysis defining crack initiation as failure would be difficult in that many airframes had some service history before fatigue testing and a portion of these aircraft already had cracks in fatigue-critical regions.
3. Some of the wings used in the RAeS analysis and also the present analysis were not cycled to complete failure. Some probable reasons were:
  - i) to reduce the time required for testing,
  - ii) inability of the test rig to cycle only one half of a wing, and
  - iii) to avoid damage to the test apparatus.

The lives of these wings were estimated by their respective researchers. These estimates were based upon the propagation rates of fatigue cracks in the specimen under consideration. Comparison with lives and crack propagation rates were also available from other specimens tested at the same load range.

4. The stresses used in the analysis were nominal or gross-section stresses in or near the fatigue-critical region. The actual stress in the initiation area was usually not known unless determined by sophisticated methods of stress analysis.
5. In general, two types of loading rigs, hydraulic and vibration, were used for fatigue testing. Ford and Payne (Ref. 4) found that in their tests on Mustang wings there was no significant difference in the variance and mean of the lives of two sets of several wings tested at the same load level in different loading rigs, one a hydraulic type and one a vibration type.
6. The precision with which loads were controlled in the various fatigue tests is unknown as not all the references discussed details of the testing methods, equipment, calibration procedures, and methods of load monitoring. This fact does add an unknown quantity of scatter to the results of the analysis.

7. It was assumed that the geometries of these various structures were similar in that being full-scale structures they all contained similar stress concentrations such as holes, rivets, bolts, hydraulic fittings, changes in section, cutouts, stiffeners, reinforcements, surface attachments, etc., all of which are potential sources of crack initiation.

### 3.2 General Comments on Fatigue Tests

Data from many structures found in the references could not be used in the analysis because of a lack of stress data for the failure locations. Probably some of this information was not published at the time of the tests for security reasons. Also, even though some references to structural fatigue tests prior to the 1950's were found, most reports from this era were either no longer in existence or not easily obtained. Other test results are probably available from the aircraft industry, such as results of tests that were published for internal use and not widely circulated.

## 4.0 ANALYSIS OF RESULTS

In the present analysis the fatigue life has been assumed to be a function of applied loads and the material (in this case either Al-Cu-Mg or Al-Zn-Mg alloy). The loads on a structure can be reduced to the form  $S_{mean} \pm S_{alt}$ ; thus, for our purposes the fatigue life can be represented by

$$N = f(S_{mean}, S_{alt}, \text{Material})$$

### 4.1 Mathematical Models

Four mathematical models were fitted to the data using the method of least-squares. The models proposed were of the following form:

$$\log_{10} N = f_1(S_m) + f_2(S_a) + f_3(M)$$

The various regression models were compared using statistics such as standard error of estimate and coefficient of correlation.

#### 4.1.1 Log N Versus Log $S_a$ Curves

The first model was:

$$\log_{10} N = b_1 + b_2 S_m + b_3 S_m^2 + b_4 S_m^3 + b_5 \log_{10} S_a$$

where  $S_m$  and  $S_a$  are in ksi. In this model  $f_1$  is a cubic polynomial in mean stress,  $f_2$  is log-linear in alternating stress, and  $f_3$  was zero as at this stage it was not yet realized that structures manufactured from different aluminum alloys would have significantly different lives. This model yielded a family of straight lines on log-log (log N vs. log  $S_a$ ) paper.

In order to reduce the number of parameters, the cubic polynomial  $f_1$  for interpolating mean stress was replaced by a logarithmic function,  $\log_{10}(S_m + 5)$ . An arbitrary constant of 5 was added to the mean stress so that the expression would be valid for  $S_m = 0$  and also could be extrapolated to mean stresses slightly less than zero if desired.

With the logarithmic interpolation for mean stress a slightly better correlation resulted, the slopes of the lines of the two models differing by less than 0.2% and the lines were almost coincident. Therefore the logarithmic function for the interpolation of mean stress was retained in all the regressions.

From the results it was also evident that there were significant differences in the lives of structures of the two material types. To account for this a dummy variable for material type was used.

The model then became

$$\log_{10} N = b_1 + b_2 \log_{10} (S_m + 5) + b_3 \log_{10} S_a + b_4 M \quad (\text{S-N Curve No. 1})$$

where

$$M = 0 \text{ for Al-Cu-Mg Alloys}$$

$$M = 1 \text{ for Al-Zn-Mg Alloys}$$

With the dummy variable, the S-N curves for the two alloys would be of similar shape, only displaced along the log N axis by the value of the coefficient of M ( $b_4$  in this case).

Figure 6 shows S-N Curve No. 1 for the Al-Cu-Mg alloy structures and Figure 7 shows S-N Curve No. 1 for the Al-Zn-Mg alloy structures.

In the next regression the term  $(\log_{10} S_a)^2$ , was added to  $f_2$ . With this quadratic term, a slightly higher coefficient of correlation was obtained. The model then became

$$\log_{10} N = b_1 + b_2 \log_{10} (S_m + 5) + b_3 \log_{10} S_a + b_4 (\log_{10} S_a)^2 + b_5 M \quad (\text{S-N Curve No. 2})$$

The resulting S-N curves were a family of parabolas on log-log paper. S-N Curve No. 2 for the Al-Cu-Mg alloy structures is shown in Figure 8 and Figure 9 shows S-N Curve No. 2 for the Al-Zn-Mg alloy structures.

The curves look unusual since they are concave downwards; however, when curves are fitted to experimental data the resulting empirical expressions may "best fit" the data but may not represent the physical process involved. The addition of a cubic term,  $(\log_{10} S_a)^3$ , did not improve the correlation.

#### 4.1.2 Log N Versus $S_a$ Curves

In these regressions  $f_2$  was represented by polynomial functions of  $S_a$ , rather than  $\log S_a$ . The mean stress was still interpolated logarithmically.

The first model of this set used a quadratic function of  $S_a$  for  $f_2$  and the expression for the S-N curve thus became

$$\log_{10} N = b_1 + b_2 \log_{10} (S_m + 5) + b_3 S_a + b_4 S_a^2 + b_5 M \quad (\text{S-N Curve No. 3})$$

The resulting curves were a set of parabolas on semi-log paper. The coefficient of correlation was slightly less than that obtained with the linear curves of log N versus  $\log S_a$ .

Figure 10 and Figure 11 show S-N Curve No. 3 for the Al-Cu-Mg and Al-Zn-Mg alloy structures respectively.

Upon studying the figures it is noticed that in the high-alternating-stress low-endurance region the curves rise sharply. This is not, of course, representative of typical S-N curves and results from the constraint of the parabolic fit. Extrapolation of the curves beyond the plotted values would lead to erroneous results.

The second model in this set included a cubic term in  $S_a$ . Thus, the model became

$$\log_{10} N = b_1 + b_2 \log_{10} (S_m + 5) + b_3 S_a + b_4 S_a^2 + b_5 S_a^3 + b_6 M \quad (\text{S-N Curve No. 4})$$

The resulting S-N curves were a set of cubics on semi-log paper. With this regression the coefficient of correlation was slightly higher than those obtained with the parabolas of  $\log N$  versus  $\log S_a$ .

S-N Curve No. 4 for the Al-Cu-Mg and Al-Zn-Mg alloy structures is shown in Figures 12 and 13 respectively.

Table 2 lists the coefficients of the parameters and some statistics obtained from the four regression models.

Further regressions were not attempted as it appeared that all four of these models yielded similar results and more complex models would only slightly increase the coefficient of correlation.

#### 4.2 Residuals

Residuals are the differences between the actual test results and the predictions from the regression equation.

Figure 14 shows the residuals plotted versus the values predicted by the regression equation for S-N Curve No. 1.

No abnormality exists if the plotted residuals form a horizontal band, rather than showing some trend such as increasing or decreasing when plotted versus the predicted value. The points in Figure 14 appear to form a horizontal band in that no other trend is noticed; thus, the least-squares analysis would not appear to be violated.

Residual plots for the other S-N curves are not included as they are similar. They can be found in Reference 16.

#### 5.0 COMPARISON OF S-N CURVES

The derived Al-Zn-Mg alloy S-N curves cannot be compared with the RAeS curves as all data used in the RAeS analysis were from Al-Cu-Mg alloy structures; however, the Al-Cu-Mg alloy curves can be compared.

Figure 15 shows S-N Curve No. 1 for Al-Cu-Mg alloys and the RAeS S-N curves superposed. Comparisons for the other curves are not shown since they are similar.

When comparing the derived Al-Cu-Mg alloy S-N curves with the RAeS curves the following generalities are noticed:

- 1) They are less conservative at high mean stresses, i.e. greater than 20 ksi.
- 2) At the lower mean stresses they are less conservative in the low-endurance high-alternating-stress region.
- 3) At the lower mean stresses they are more conservative in the high-endurance low-alternating-stress region.

In conjunction with the above three statements the following should also be taken into consideration:

- 1) Mean stresses greater than 20 ksi are rare in practice.
- 2) The frequency of loads in the low-endurance high-alternating-stress region is low; thus, their effect on fatigue life (using a linear damage rule) is negligible.
- 3) The frequency of loads in the high-endurance low-alternating-stress region is high; therefore, the fatigue life can be significantly affected by the S-N curves in this region.

From the preceding items it can be concluded that any major differences in fatigue life calculations using these derived S-N curves as opposed to the RAeS curves will be primarily due to high-frequency low-amplitude loads.

## 6.0 SCATTER IN CONSTANT-AMPLITUDE FATIGUE DATA

The standard deviation of log life of the pooled data is approximately the same for all the derived S-N curves ( $\cong 0.35$ ); therefore, any of the derived S-N curves will predict lives of constant-amplitude tests with approximately the same reliability.

This large scatter, i.e. about three times as great as the scatter normally found in replicate tests on nominally identical structures, is due to the superposition of scatter from two sources: the first is the scatter inherent in a single type of aircraft structure and the second is the scatter due to combining several types of aircraft structures.

### 6.1 Scatter Within a Group of Similar Structures

Within a set of similar items scatter can be caused by construction variations, slightly different material properties due to heat-to-heat variation, and residual stresses induced during fabrication.

### 6.2 Scatter Due to Different Types of Structures

There are gross material differences among aircraft structures of different types, the only allowance made for material type was for differences between two of the major groups, namely aluminum-copper-magnesium alloys and aluminum-zinc-magnesium alloys. Within these groups the material properties and heat treatments can vary widely.

Also, the types of structures included in this analysis varied considerably. Included were aircraft ranging in size from fighters to transports. Elements tested were wings, major sections of wings, and vertical and horizontal tailplanes. This variety alone suggests that considerable scatter in the results is to be expected.

All of the effects contributing to scatter in the above two sections were combined and hence the reason for the large scatter.

The magnitude of the scatter can best be appreciated by reference to Figure 16. Shown for S-N Curve No. 1 are the actual lives versus predicted lives for the 246 constant-amplitude tests. The standard error of estimate is  $\cong 0.35$ . The  $\pm 2\sigma$  limits are drawn on Figure 16 and 95.5% of the points are expected to be within these limits if the distribution is assumed to be log normal. It is noticed that in the graph only eight points are outside the  $\pm 2\sigma$  limits which is somewhat better than is predicted using the log-normal distribution. Graphs for the other curves are very similar and thus are not shown. The maximum number of points outside the  $\pm 2\sigma$  limits on any graph is eight.

## 7.0 LIFE PREDICTIONS USING VARIOUS S-N CURVES AND RELIABILITY OF PREDICTIONS

### 7.1 Lives Predicted by Various S-N Curves

The lives of several aircraft tested under programmed loading were compared with the predicted lives calculated using Miner's Rule in conjunction with the RAeS S-N curves and the S-N curves derived from the regressions.

As the life calculations were computerized, mathematical expressions were also required for the RAeS curves. Sewell (Ref. 17) proposed a model which fits the RAeS curves very closely for mean stresses between 2 and 20 ksi and Douglas (Ref. 18) proposed a model which covers the range of mean stress from 0 to 30 ksi. Douglas uses Sewell's method between 2 and 15 ksi mean stress. These expressions are shown in Appendix I.

Life calculations were made using the four derived S-N curves and both Douglas' and Sewell's expressions for the RAeS S-N curves.

Table 3 contains the list of aircraft for which lives of wing or tail structures were calculated and the references from which the information was taken. The eight aircraft yielded a total of 18 test cases for which lives could be computed. A summary of the life calculations is shown in Tables 4 and 5. Further details on the calculations, the loads spectra and stresses are given in Reference 16. Appendix II shows a computer printout of a typical life calculation.

Tables 4 and 5 show the actual lives (log mean if more than one structure was tested), the calculated lives as predicted by each S-N curve and the damage ratios  $\left( \sum \frac{n}{N} = \frac{\text{actual life}}{\text{calc. life}} \right)$ . Where more than one structure was tested, the log standard deviation was also calculated in order to obtain an appreciation of the scatter within a group of similar structures.

It was noticed that the greatest scatter occurred in the Mustang wings and Commando wings which are relatively old structures. Scatter in newer structures appears to be less.

The damage ratios for each of the four derived S-N curves were plotted on probability paper and compared with the damage ratios obtained using the RAeS curves. These plots are shown in Figures 17, 18, 19 and 20. These figures show that in all four cases the derived S-N curves give results which are less scattered and more conservative than predictions using the RAeS S-N curves. Similar diagrams comparing the two mathematical expressions for the RAeS S-N curves were not made as in only two cases (U.S. Jet Fighter Spectra 1 and 2) were there any differences in the calculated lives. In these cases Douglas' method was slightly more accurate than Sewell's method.

Table 6 is a summary of the life calculations shown in Tables 4 and 5. In Table 6 are the minimum damage ratios, maximum damage ratios, the ratios of maximum to minimum, the number of unconservative predictions  $\left( \sum \frac{n}{N} < 1 \right)$ , the log means of the damage ratios, the log standard deviations of the damage ratios, the damage ratios at  $-3\sigma$  from the mean, and the probabilities of survival at  $\sum \frac{n}{N} = 1$  for each S-N curve.

The last three columns of this table show that the new curves are a definite improvement over the existing curves. The log standard deviation for the RAeS curves is  $\approx 0.38$  while for the derived curves they range from 0.19 to 0.22, i.e. almost half the value. As a result, this yields higher allowable damage ratios for equal reliability (e.g.  $-3\sigma$ ) and higher confidence at any damage ratio

(e.g.  $\sum \frac{n}{N} = 1$ ) for the derived S-N curves.

It is noticed that the log means of all the damage ratios are greater than unity and that the log standard deviations ( $\approx 0.19$  to  $0.22$  for the derived curves) for the variable-amplitude tests are less than the log standard deviations from the constant-amplitude tests ( $\approx 0.35$ ). Both of these facts are probably the result of load interactions.

## 7.2 Reliability of Predictions

It is essential for the user of any of these curves to have an estimate of the reliability of the life calculation. As mentioned, means and standard deviations of the damage ratios were calculated for each S-N curve and are shown in Table 6. From these, the reliability of any life prediction at  $\sum \frac{n}{N} = 1$  can be estimated. Also estimated can be the values of  $\sum \frac{n}{N}$  for the S-N curves such that they have the same reliability.

Let  $M_1$ , see Figure 21, be the mean of the various aircraft structures. Unless several full-scale tests are performed on the wing structure in question, it is not known where the actual life lies in Distribution No. 1. Therefore, to be conservative one must move down on this distribution, for example  $3\sigma_1$ , to  $M_2$ .

This point  $M_2$  is then assumed to be the mean life of a fleet of aircraft. The fatigue lives of aircraft within this fleet are distributed about  $M_2$  and have a log standard deviation  $\sigma_2$ . A value for  $\sigma_2$  was estimated using the 14 log standard deviations shown in Tables 4 and 5 and the following formula:

$$\sigma = \left[ \frac{S_1^2 n_1 + S_2^2 n_2 + \dots + S_k^2 n_k}{n_1 + n_2 + \dots + n_k - k} \right]^{1/2}$$

where

$S_i$  = log standard deviation of group  $i$

$M_i$  = number of specimens in group  $i$

$k$  = number of groups

The value obtained for the composite log standard deviation was 0.104. This is in agreement with Impellizzeri's (Ref. 26) findings which also suggest a log standard deviation of the order of 0.10. Thus, it was decided to use a value of 0.10 for  $\sigma_2$ . To obtain a satisfactory degree of reliability for the fleet one must move down, say for example  $3\sigma_2$ , on Distribution No. 2.

The numbers below the  $\sum \frac{n}{N}$  axis (Fig. 21) are the values of  $\sum \frac{n}{N}$  for the various S-N curves that yield the same level of reliability. It is, of course, up to the individual user of these S-N curves to decide what degree of reliability is desired.

The rightmost column contains the scatter factors needed for the various S-N curves if  $-3\sigma$  is an acceptably safe limit on each distribution and Miner's Rule ( $\sum \frac{n}{N} = 1$  at failure) is used.

The combination of these two factors ( $-3\sigma$  on each distribution) gives a probability of failure of  $(1 - 0.99865)^2$  or  $\approx 2 \times 10^{-6}$  and then for a fleet size of  $n$ , the expected loss is  $\approx 2n \times 10^{-6}$  aircraft. The probability of failure of in-service aircraft and hence the expected loss is also a function of the frequency of inspection and maintenance, inspection techniques and operator skill, and the certainty with which the fatigue-critical location is known. The overall probability of failure, therefore, cannot easily be quantified.

## 8.0 CONCLUSIONS

- 1) Any one of the four derived S-N curves predicts fatigue life of aluminum aircraft wing structures more reliably than the RAeS S-N curves. S-N Curves Nos. 2 and 4 give the most reliable predictions.

It is felt that S-N Curve No. 4 is the best curve taking into consideration its shape and the statistics summarized in Tables 2 and 6.

- 2) Any major difference in fatigue life calculations using the derived S-N curves as opposed to the RAeS S-N curves will be primarily due to high-frequency low-amplitude loads.
- 3) Structures manufactured from zinc-bearing aluminum alloys appear to have significantly shorter fatigue lives (3-1/2 to 4 times shorter on the average) than structures manufactured from copper-bearing aluminum alloys.
- 4) For pooled data from various aircraft the scatter in variable-amplitude tests is less than the scatter in constant-amplitude tests. For the constant-amplitude tests the log standard error of estimate was approximately 0.35 and the log standard deviation for the variable-amplitude tests using the derived curves was of the order of 0.2.
- 5) The scatter within any one group of aircraft structures is considerably smaller than for the pooled data. The composite log standard deviation of several tests was  $\cong 0.10$ . The more modern structures appear to exhibit less scatter than the older structures, presumably due to tighter quality control of materials and manufacturing processes.

## 9.0 REFERENCES

1. Royal Aeronautical Society      *Data Sheets — Fatigue.*  
Vol. 1, Sheet E.02.01, June 1962.
2. Raithby, K.D.                      *Fatigue Tests on Typical Two Spar Light Alloy Structures*  
*(Meteor 4 Tailplanes).*  
ARC Current Paper 88, 1952.
3. Raithby, K.D.                      *Some Fatigue Characteristics of a Two Spar Light Alloy Structure*  
Longson, J.                              *(Meteor 4 Tailplane).*  
ARC Current Paper 258, 1956.
4. Ford, D.G.                              *Fatigue Characteristics of a Riveted 24S-T Aluminium Alloy*  
Payne, A.O.                              *Wing Part IV. Analysis of Results.*  
ARL Report SM 263, Dept. of Supply, Melbourne, October  
1958.
5. McGuigan Jr., M.J.                      *Fatigue Investigation of Full-Scale Transport-Airplane Wings.*  
Bryan, D.F.                              *Summary of Constant-Amplitude Tests Through 1953.*  
Whaley, R.E.                              NACA TN 3190, March 1954.
6. Whaley, R.E.                              *Fatigue Investigation of Full-Scale Transport-Airplane Wings.*  
*Variable-Amplitude Tests with Gust-Loads Spectrum.*  
NACA TN 4132, November 1957.
7. Foster Jr., L.R.                              *Fatigue Investigation of Full-Scale Transport-Airplane Wings.*  
Whaley, R.E.                              *Tests with Constant-Amplitude and Variable-Amplitude*  
*Loading Schedules.*  
NASA Technical Note D-457, October 1960.

8. Winkworth, W.J. *Fatigue Behaviour Under Service and Ground Test Conditions (A Comparison Based on the Dakota Wing).*  
ARC Current Paper 666, 1964.
9. Raithby, K.D. *Fatigue Testing of a Large Wing by the Resonance Method.*  
RAE Report No. Structures 150, Farnborough, August 1953.
10. Carl, R.A.  
Wegend, T.J. *Investigations Concerning the Fatigue of Aircraft Structures.*  
ASTM Proceedings, Vol. 54, 1954, p. 903.
11. Rosenfeld, M.S. *Aircraft Structural Fatigue Research in the Navy.*  
ASTM STP 338, Symposium on Fatigue of Aircraft Structures, 1962, p. 216.
12. Swartz, R.P.  
Rosenfeld, M.S. *Constant Amplitude Fatigue Characteristics of a Slab Horizontal Tail for a Typical Fighter Airplane.*  
U.S. Naval Air Material Center, Report No. NAMATCEN-ASL-1023, Part I, January 1960.
13. Zoudlik, R.J.  
Rosenfeld, M.S. *Constant Amplitude Fatigue Characteristics of a Vertical Tail for a Typical Fighter Airplane.*  
U.S. Naval Air Material Center, Report No. ASL-1049, Part I, March 1962.
14. Ditchfield, C. *Fatigue Life of the C-100 Mk 4 and Mk 5 Aircraft.*  
Avro Aircraft Ltd., C-100/A/404, Issue C, December 1959.
15. Schijve, J.  
de Rijk, P. *Fatigue Test Results of Three Full-Scale Wing Center Sections Under Constant-Amplitude Loading.*  
NLR-TM S.640, Amsterdam, November 1965.
16. Hangartner, R. *S-N Curves for Fatigue Life Prediction of Aluminum Aircraft Wing Structures.*  
Master's Thesis, University of Waterloo, Waterloo, Ontario, August 1974.
17. Sewell, R. T. *An Investigation of Flight Loads, Counting Methods, and Effects on Estimated Fatigue Life.*  
SAE Paper 720305, March 1972.
18. Douglas, R.B. *An Investigation of Methods of Interpolating Between S-N Curves for the Endurance of Complete Wings and Tailplanes at Different Mean Stresses.*  
Department of Civil Aviation, Aeronautical Engineering Report SM-64, Australia, August 1972.
19. Parish, H.E. *Fatigue Test Results and Analysis of 42 Piston Provost Wings.*  
ARC R & M No. 3474, April 1965.
20. Payne, A.O. *Random and Programmed Load Sequence Fatigue Tests on 24S-T Aluminium Alloy Wings.*  
ARL Report SM 244, Dept. of Supply, Melbourne, September 1956.
21. Jost, G.S.  
Lewis, J.Y. *A Comparison of Experimental and Predicted Fatigue Lives of Mustang Wings Under Programmed and Random Loading.*  
ARL Report SM 300, Dept. of Supply, Melbourne, December 1964.

22. Patching, C.A.  
Mann, J.Y. *Comparison of a 2L.65 Aluminium Alloy Structure with Notched Specimens Under Programmed and Random Fatigue Loading Sequences.*  
Fatigue Design Procedures, Proceedings of the 4th ICAF Symposium, Edited by Gassner and Schütz, Munich 1965.
23. Dunsby, J.A.  
Pinkney, H.F.L.  
Sewell, R.T.  
Barszczewski, A. *Fatigue Life Prediction of the CF-100 Aircraft.*  
NRC, Aeronautical Report LR-438, National Research Council of Canada, Ottawa, Ontario, August 1965.
24. Swartz, R.P.  
Rosenfeld, M.S. *Variable Amplitude Fatigue Characteristics of a Slab Horizontal Tail for a Typical Fighter Airplane.*  
U.S. Naval Air Material Center Report No. NAMATCEN-ASL-1023, Part II, September 1961.
25. Schijve, J.  
Broek, D.  
de Rijk, P.  
Nederveen, A.  
Sevenhuysen, P.J. *Fatigue Tests With Random and Programmed Load Sequences With and Without Ground-to-Air Cycles. A Comparative Study on Full-Scale Wing Center Sections.*  
NLR-TR S.613, Amsterdam, December 1965.
26. Impellizzeri, L.F. *Development of a Scatter Factor Applicable to Aircraft Fatigue Life.*  
ASTM STP 404, Structural Fatigue in Aircraft, 1966, p. 136.

TABLE 1

CONSTANT-AMPLITUDE DATA USED IN ANALYSIS

Aircraft Type and Component	No. of Tests	Reference
Meteor 4 Tailplane	36	2 and 3
P51D Mustang Wing	124	4
C-46 Commando Wing	18	5, 6, and 7
Dakota Wing	2	8
Lancaster Wing	1	9
Piston Aircraft* Outer Wing Panels	5	10
Piston Fighter* Wings	2	10
Jet Aircraft* Outer Wing Panels	7	10
F3H-1 Horizontal Tails	19	11 and 12
F3H-1 Vertical Tails	20	11 and 13
CF-100 Wings	9	14
Fokker F27 Wing Centre Section	<u>3</u>	15
Total Tests	246	

\* Aircraft type not disclosed in reference.

**TABLE 2**  
**RESULTS OF VARIOUS REGRESSIONS**

	Coefficients						Statistics			
	Constant	$\text{Log}_{10} (S_m + 5)$	$\text{Log}_{10} S_a$	$(\text{Log}_{10} S_a)^2$	M	$\Sigma e^2$ $\Sigma \text{ Errors Squared}$	Standard Error of Estimate	R Coefficient of Correlation	$R^2$	
S-N Curve No. 1	8.74689	-1.08497	-2.93236	-	-0.577039	30.5450	0.355273	0.92538	0.85663	
S-N Curve No. 2	8.22984	-1.11834	-1.46396	-0.882192	-0.555914	29.3274	0.348842	0.92816	0.8615	
	Coefficients									
	Constant	$\text{Log}_{10} (S_m + 5)$	$S_a$	$S_a^2$	$S_a^3$	M				
S-N Curve No. 3	7.99274	-1.11862	-0.259901	$0.503694 \times 10^{-2}$	-	-0.532048	30.7587	0.357253	0.92451	0.8547
S-N Curve No. 4	8.37374	-1.11813	-0.389103	$0.164425 \times 10^{-1}$	$-0.280037 \times 10^{-3}$	-0.547449	29.0687	0.348022	0.92851	0.8621

TABLE 3

VARIABLE-AMPLITUDE TESTS

Aircraft	Reference
Piston Provost	19
P51D Mustang	20 and 21
Vampire	22
C-46 Commando	6 and 7
U.S. Navy Jet Fighter	10
CF-100	23
F3H-1	11 and 24
Fokker F27	25

TABLE 4  
 LIFE PREDICTIONS RESULTING FROM THE USE OF VARIOUS S-N CURVES  
 COMPARED WITH LOG MEANS OF ACTUAL TESTS. Al-Cu-Mg Alloy Structures

Aircraft	Log Mean of Test Lives	$\sigma$ Log N	No. of Tests	RAeS (Sewell)		RAeS (Douglas)		S-N Curve No. 1		S-N Curve No. 2		S-N Curve No. 3		S-N Curve No. 4	
				Calc. Life	$\frac{n}{\Sigma N}$	Calc. Life	$\frac{n}{\Sigma N}$	Calc. Life	$\frac{n}{\Sigma N}$	Calc. Life	$\frac{n}{\Sigma N}$	Calc. Life	$\frac{n}{\Sigma N}$	Calc. Life	$\frac{n}{\Sigma N}$
Piston Provost Wings Hi-Lo Sequence	9452 hours	0.087	41	1993	4.74	1993	4.74	3724	2.54	3634	2.60	3479	2.72	3602	2.62
Piston Provost Wings Lo-Hi Sequence	7900 hours	0.083	11	1993	3.96	1993	3.96	3724	2.12	3634	2.17	3479	2.27	3602	2.19
Mustang Wings Gun-Bay Area	45.69 blocks	0.158	4	12.1	3.78	12.1	3.78	12.8	3.57	13.0	3.51	13.0	3.51	13.6	3.36
Mustang Wings Tank-Bay Area	36.31 blocks	0.169	7	46.7	0.78	46.7	0.78	34.7	1.05	31.4	1.16	27.0	1.34	32.1	1.13
Vampire Jet Trainer	115.75 blocks	0.062	16	71.2	1.63	71.2	1.63	102	1.13	103	1.12	99.0	1.17	101	1.15
Commando Wings Gust Loads 4.85 ksi/g	125.6 blocks	0.101	8	660	0.19	660	0.19	183	0.69	106	1.18	52.8	2.38	83.5	1.50
Commando Wings Gust Loads 5.53 ksi/g	218 blocks	-	1	328	0.66	328	0.66	116	1.88	76.3	2.86	43.1	5.06	64.4	3.39
Commando Wings Gust Loads 6.16 ksi/g	174 blocks	-	1	184	0.95	184	0.95	79.4	2.19	57.2	3.04	35.8	4.86	50.9	3.42
Commando Wings Manoeuvre Loads 4.85 ksi/g	30.3 blocks	0.071	2	26.9	1.13	26.9	1.13	17.3	1.75	17.9	1.69	17.1	1.77	17.8	1.70
Commando Wings Manoeuvre Loads 6.57 ksi/g	17.3 blocks	0.225	2	5.54	3.12	5.54	3.12	5.98	2.89	6.35	2.72	6.44	2.69	6.18	2.80

TABLE 5  
 LIFE PREDICTIONS RESULTING FROM THE USE OF VARIOUS S-N CURVES  
 COMPARED WITH LOG MEANS OF ACTUAL TESTS. Al-Zn-Mg Alloy Structures

Aircraft	Log Mean of Test Lives	$\sigma_{\log N}$	No. of Tests	RAeS (Sewell)		RAeS (Douglas)		S-N Curve No. 1		S-N Curve No. 2		S-N Curve No. 3		S-N Curve No. 4	
				Calc. Life	$\Sigma \frac{n}{N}$	Calc. Life	$\Sigma \frac{n}{N}$	Calc. Life	$\Sigma \frac{n}{N}$	Calc. Life	$\Sigma \frac{n}{N}$	Calc. Life	$\Sigma \frac{n}{N}$	Calc. Life	$\Sigma \frac{n}{N}$
U.S. Jet Fighter Spectrum No. 1	23.9 blocks	0.054	2	10.6	2.25	12.7	1.88	7.66	3.12	6.91	3.46	6.63	3.60	7.45	3.21
U.S. Jet Fighter Spectrum No. 2	872 blocks	0.028	2	391	2.23	443	1.97	245	3.56	240	3.63	242	3.60	246	3.54
CF-100	24150 hours	—	1	92914	0.26	92914	0.26	21844	1.11	23418	1.03	24298	0.99	24607	0.98
F3H-1 Horizontal Tail Spectrum No. 1	121.4 blocks	0.120	3	92.0	1.32	91.7	1.32	43.1	2.82	47.6	2.55	51.5	2.36	46.1	2.63
F3H-1 Horizontal Tail Spectrum No. 2	165.9 blocks	0.114	3	86.6	1.92	86.3	1.92	38.3	4.33	42.4	3.91	46.1	3.60	41.6	3.99
F3H-1 Horizontal Tail Spectrum No. 3	95.6 blocks	0.092	3	90.1	1.06	89.8	1.06	40.2	2.38	43.7	2.19	46.3	2.06	42.6	2.24
F3H-1 Horizontal Tail Spectrum No. 4	81.1 blocks	0.081	3	95.7	0.85	95.4	0.85	41.1	1.97	46.1	1.76	50.9	1.59	45.1	1.80
Fokker F27	50.5 blocks	—	1	36.4	1.39	36.4	1.39	14.1	3.58	15.5	3.26	16.9	2.99	15.7	3.22

TABLE 6  
 SUMMARY OF DAMAGE RATIOS OF LIFE PREDICTIONS USING VARIOUS S-N CURVES

S-N Curve	Min. $\Sigma \frac{n}{N}$	Max. $\Sigma \frac{n}{N}$	Ratio $\frac{\max}{\min}$	No. of $\Sigma \frac{n}{N} < 1$ Out of 18 Tests	Log-Mean $\frac{n}{\Sigma N}$	$\sigma$ (log)	$\Sigma \frac{n}{N}$ for $-3\sigma$	Probability of Mean Life $>$ Predicted @ $\Sigma \frac{n}{N} = 1$
RAeS (Sewell)	0.19	4.74	24.9	6	1.32	0.379	0.10	63%
RAeS (Douglas)	0.19	4.74	24.9	6	1.30	0.375	0.10	62%
S-N Curve No. 1	0.69	4.33	6.28	1	2.13	0.219	0.47	93%
S-N Curve No. 2	1.03	3.91	3.80	0	2.24	0.193	0.59	96%
S-N Curve No. 3	0.99	5.06	5.11	1	2.45	0.202	0.61	97%
S-N Curve No. 4	0.98	3.99	4.07	1	2.30	0.191	0.61	97%

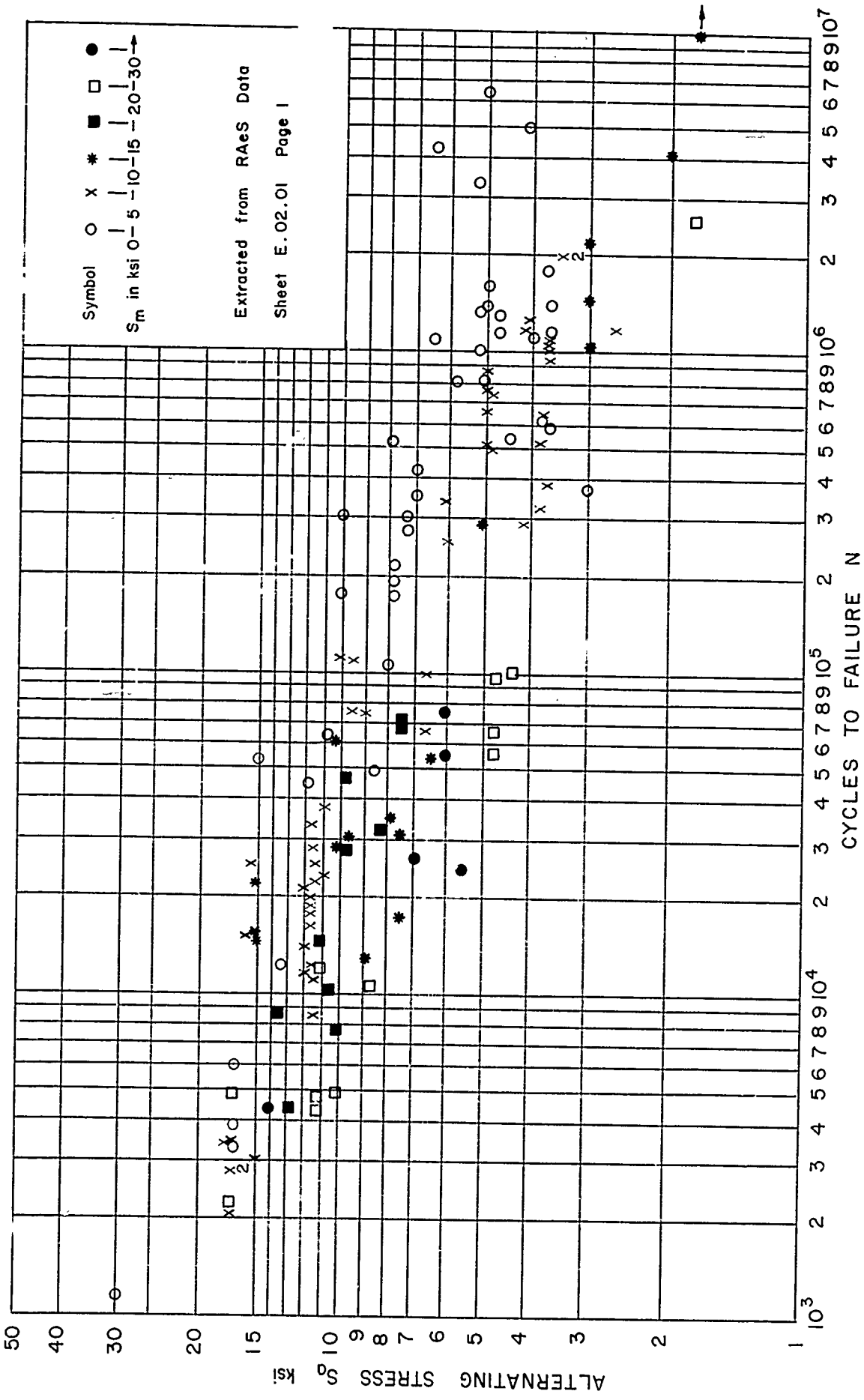


FIG. 1: EXPERIMENTAL DATA

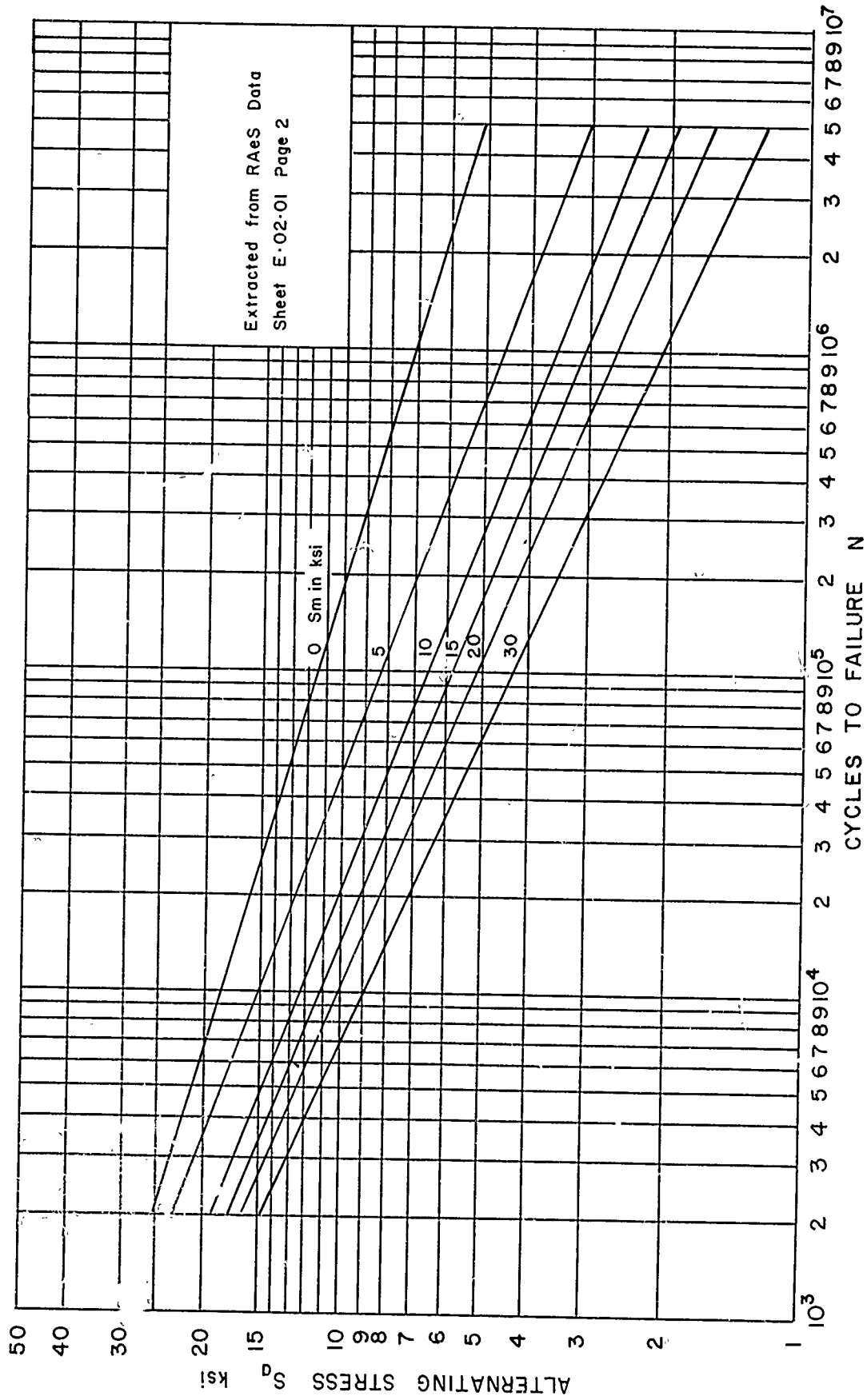


FIG. 2: AVERAGE ENDURANCES OF COMPLETE WINGS AND TAILPLANES

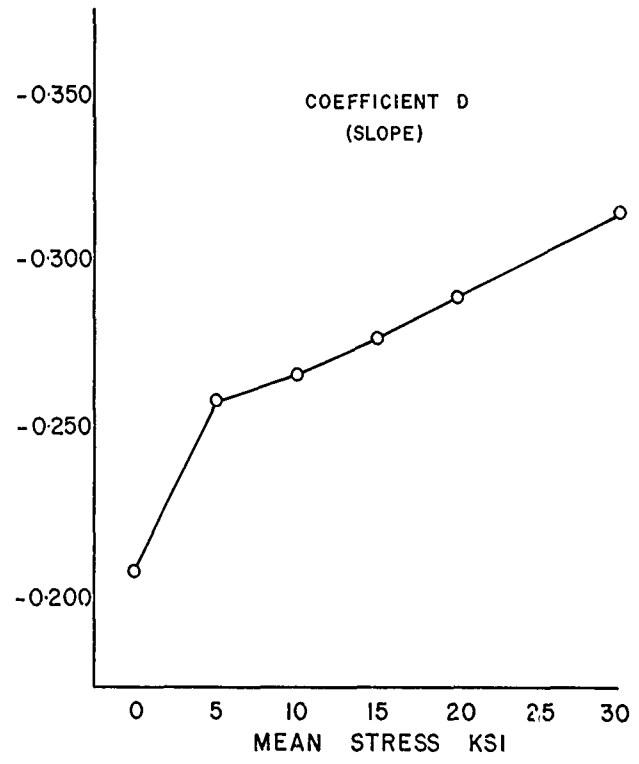
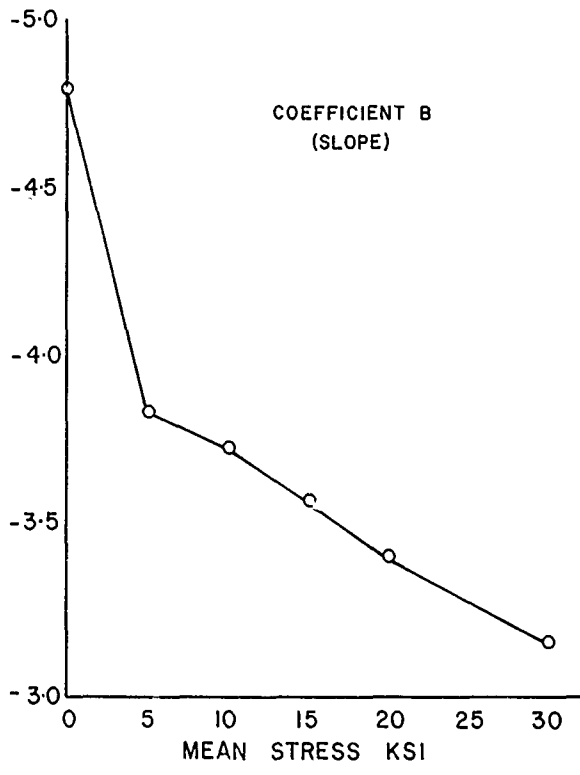
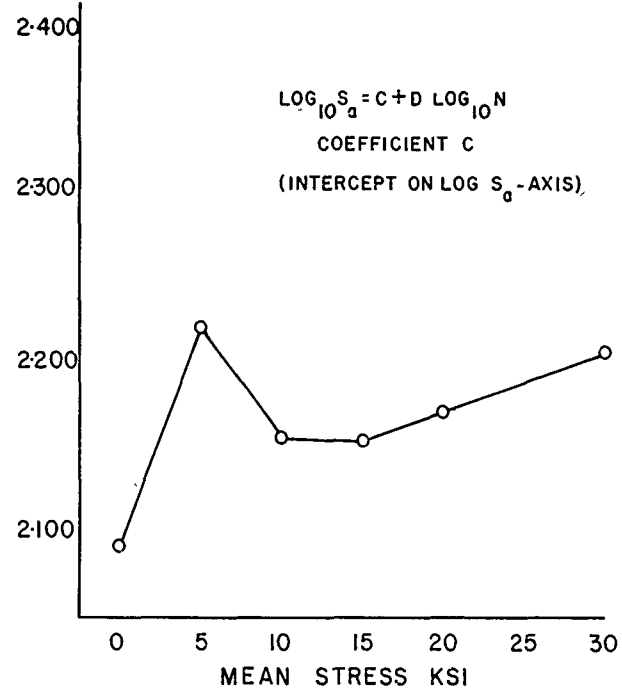
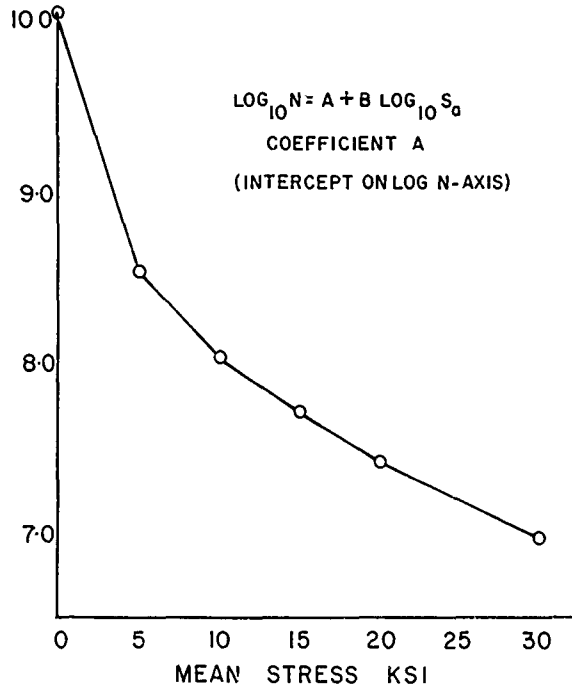
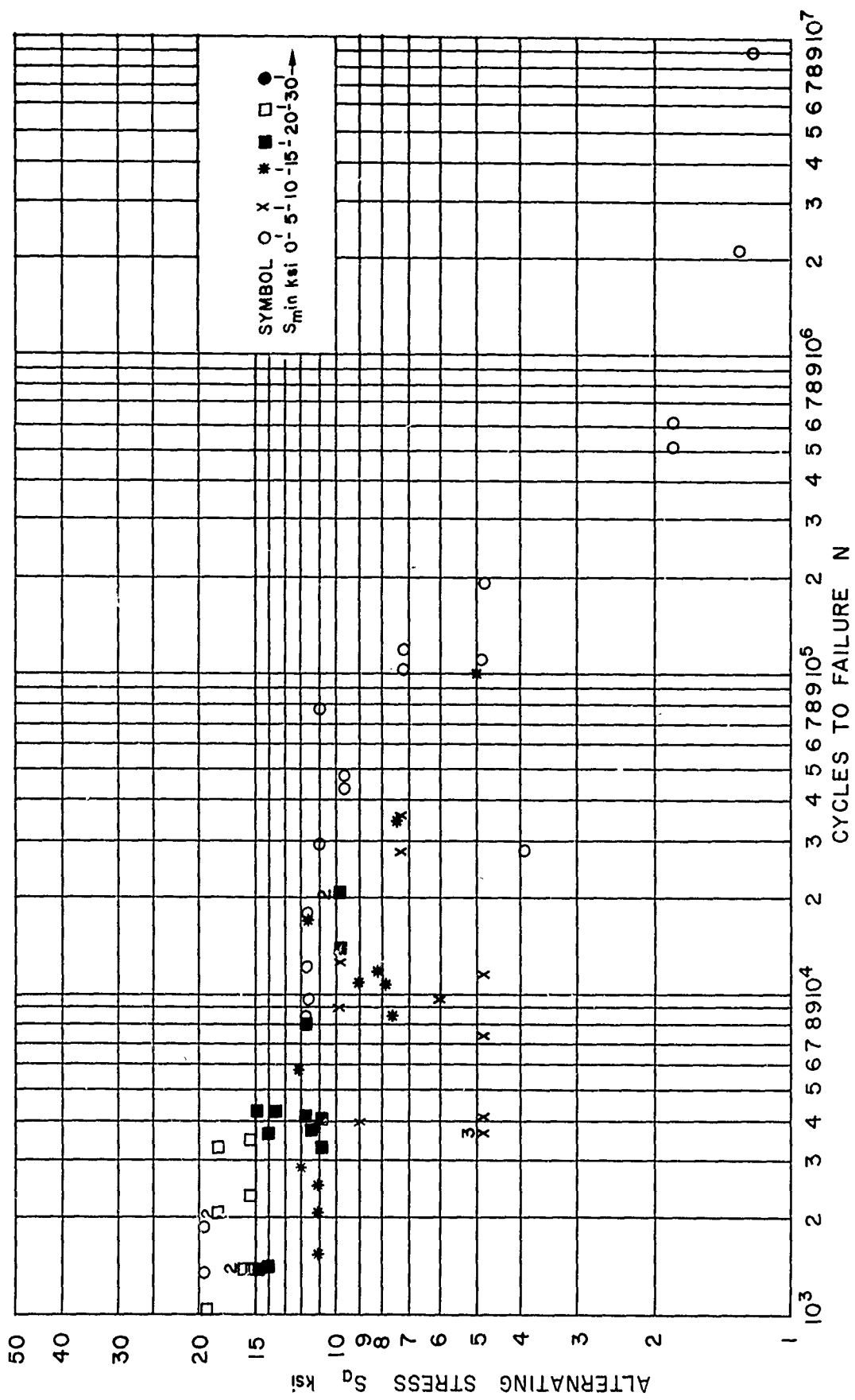


FIG. 3: COEFFICIENTS OF EQUATIONS REPRESENTING  
 RAeS S-N CURVES VS. MEAN STRESS





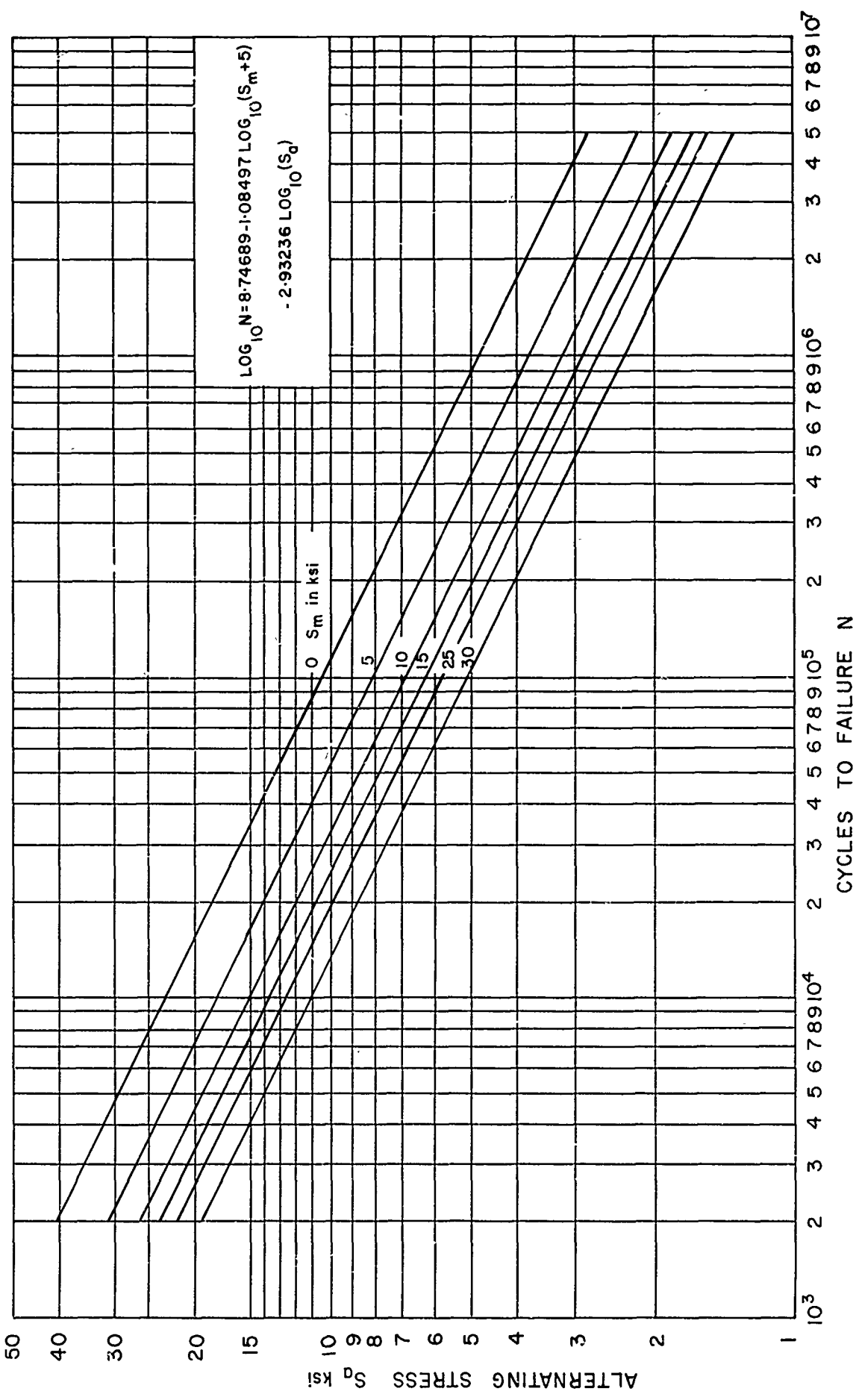


FIG. 6: S-N CURVE No.1, Al-Cu-Mg ALLOY STRUCTURES, LINEAR S-N CURVE

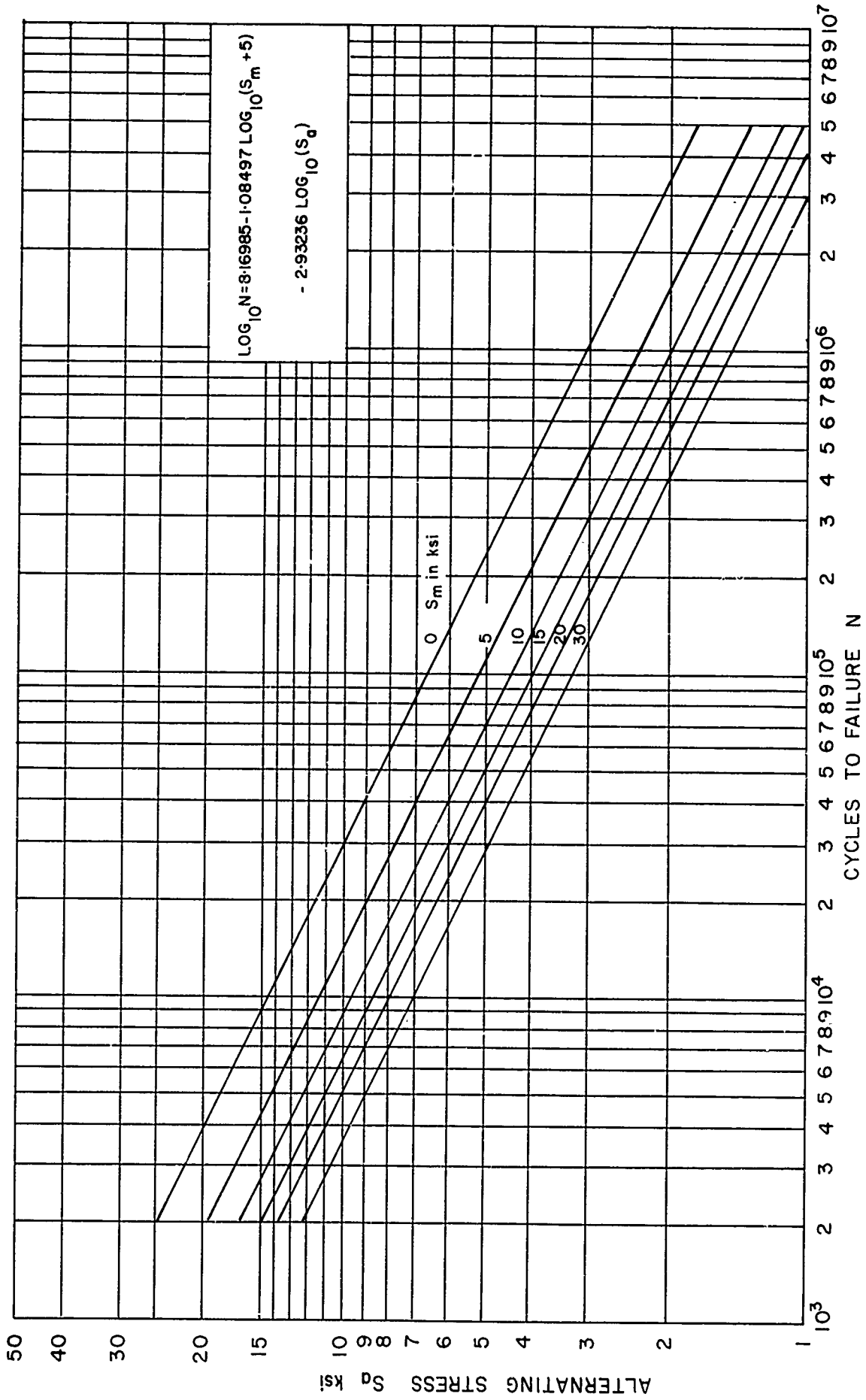


FIG. 7: S-N CURVE NO. 1, Al-Zn-Mg ALLOY STRUCTURES, LINEAR S - N CURVE

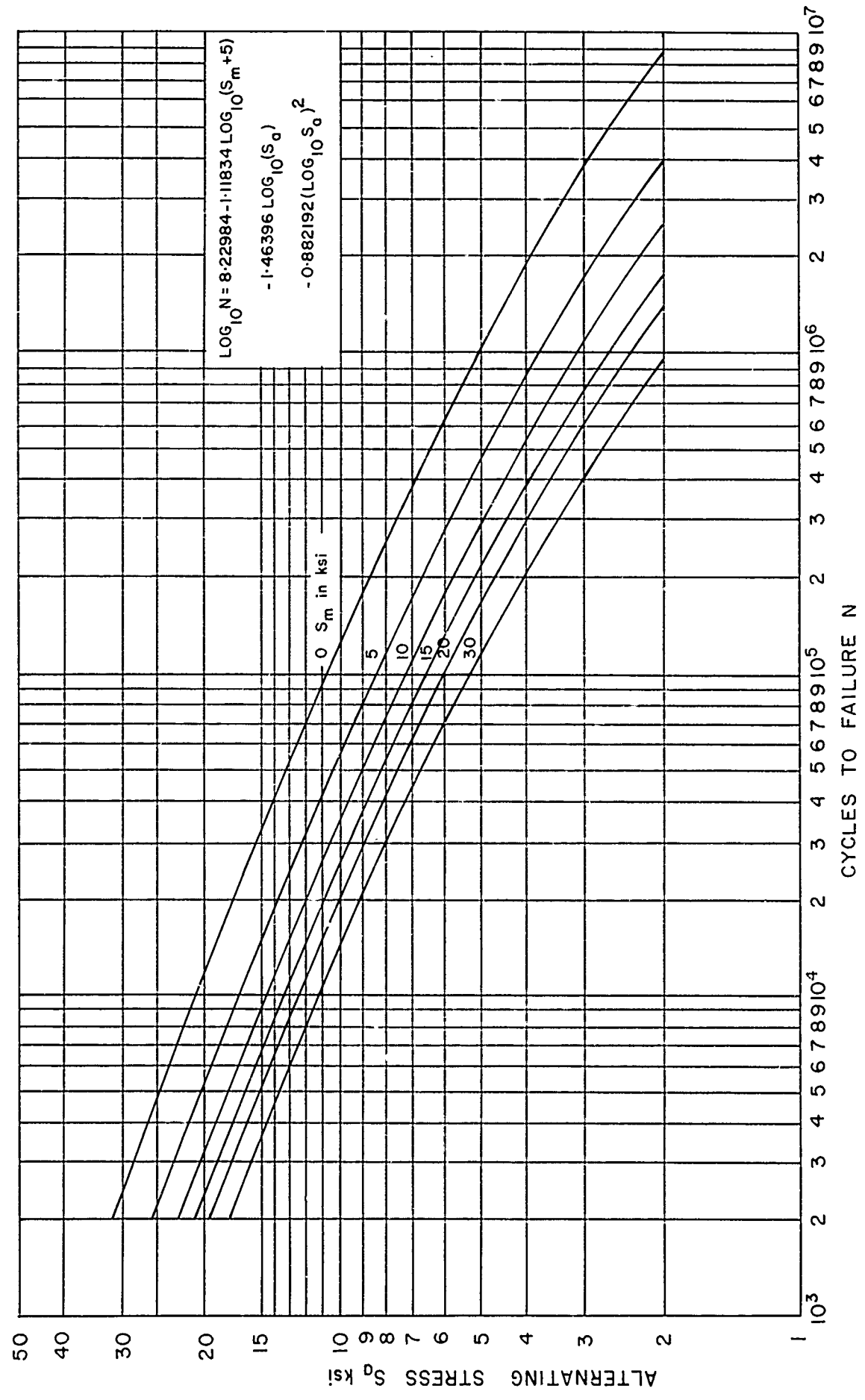


FIG. 8: S-N CURVE NO.2, Al-Cu-Mg ALLOY STRUCTURES, QUADRATIC S-N CURVE

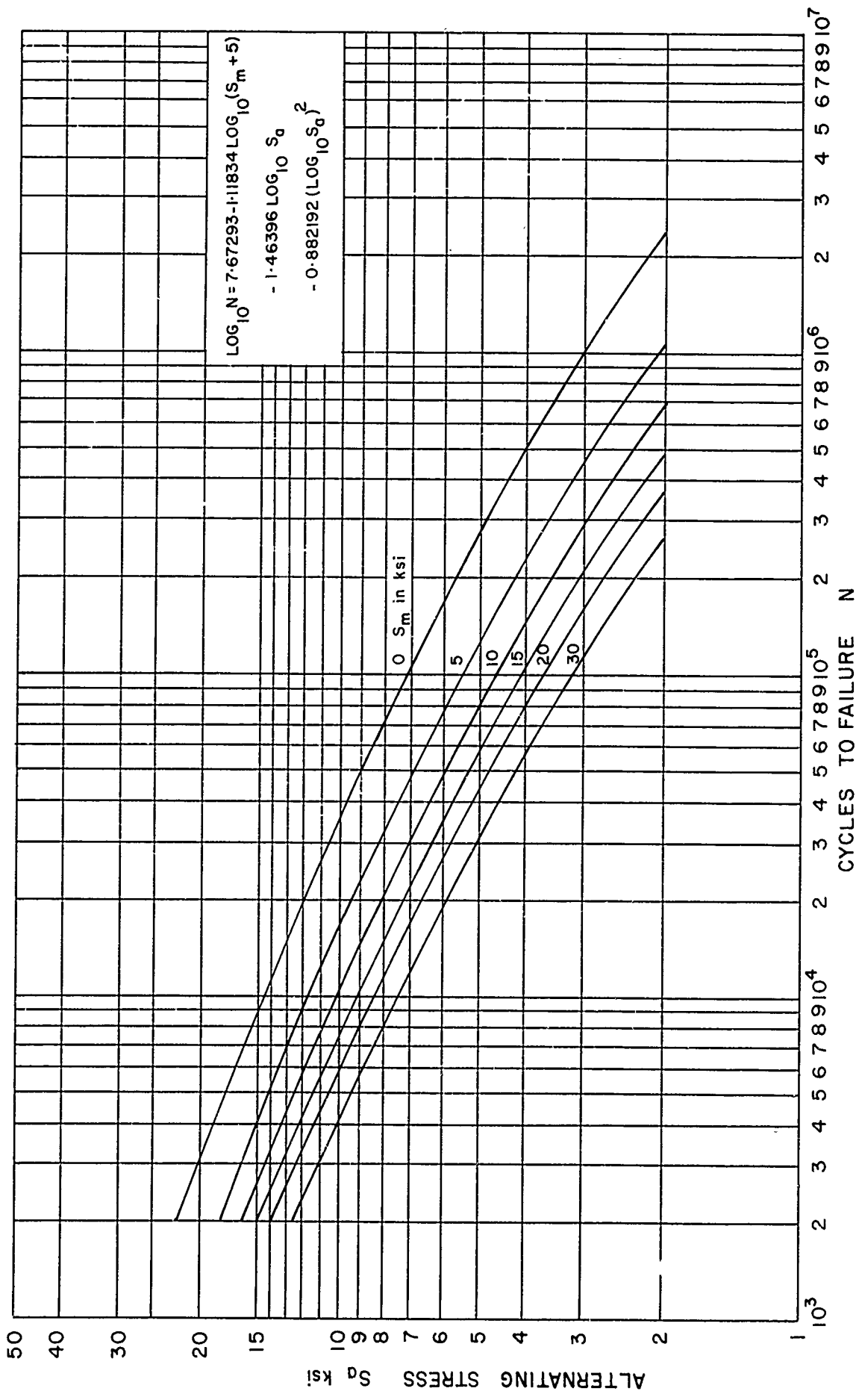


FIG. 9: S-N CURVE NO. 2, Al-Zn-Mg ALLOY STRUCTURES, QUADRATIC S-N CURVE

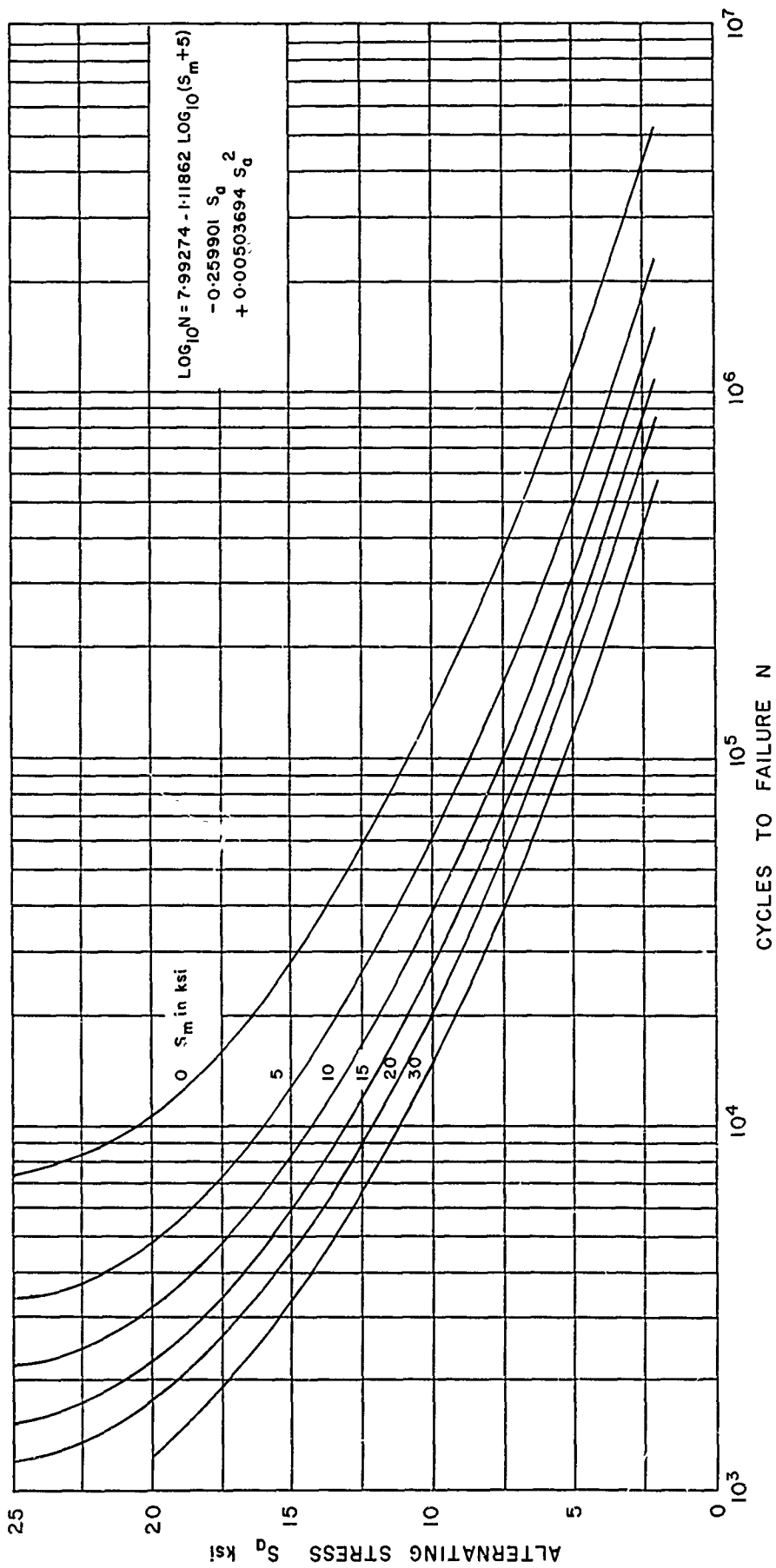


FIG. 10: S-N CURVE NO. 3, Al-Cu-Mg ALLOY STRUCTURES, QUADRATIC S-N CURVE

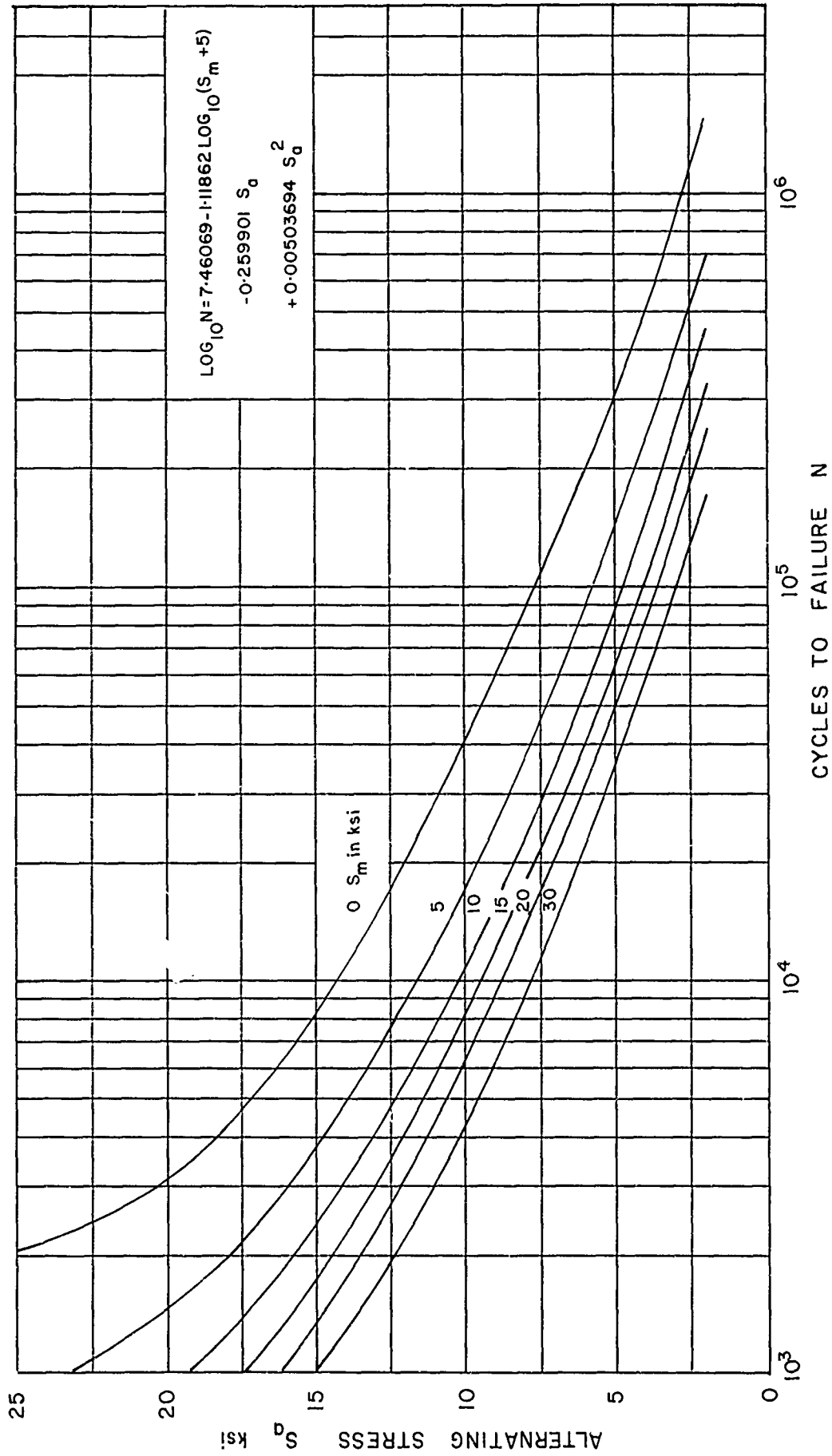


FIG. 11: S-N CURVE NO. 3, Al-Zn-Mg ALLOY STRUCTURES, QUADRATIC S-N CURVE

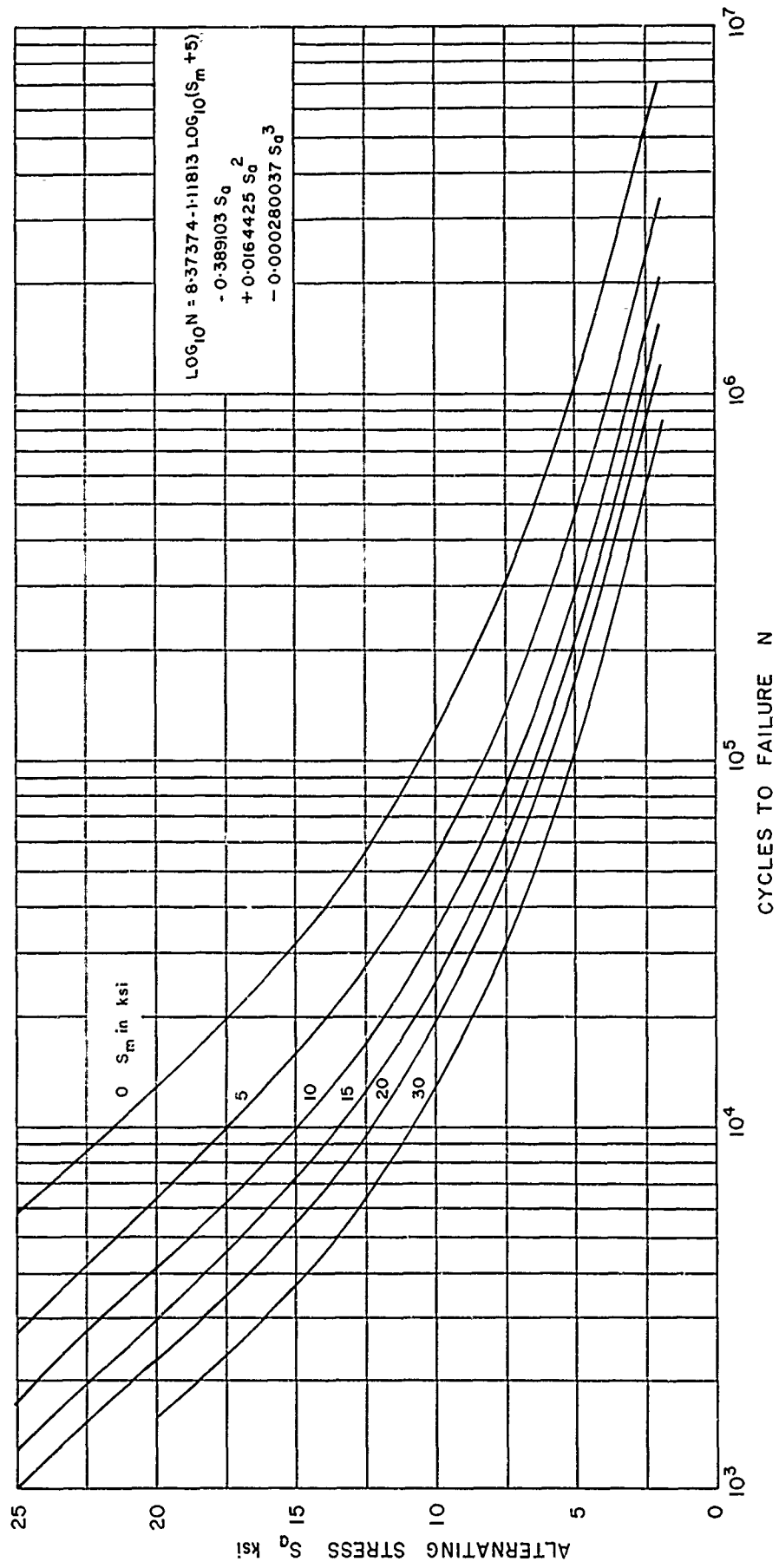


FIG. 12: S-N CURVE NO. 4, Al-Cu-Mg ALLOY STRUCTURES, CUBIC S-N CURVE

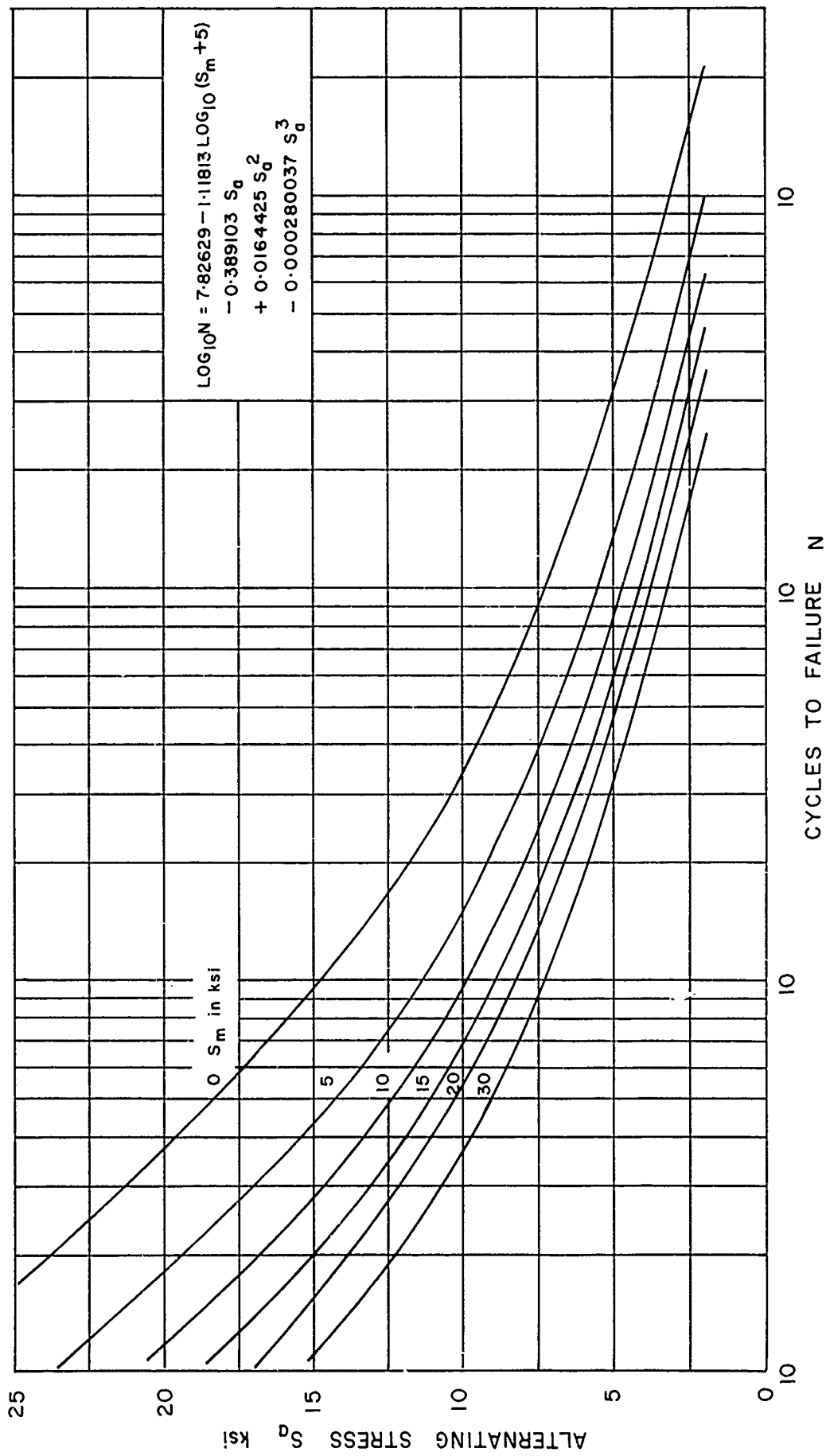


FIG. 13: S-N CURVE NO. 4, Al-Zn-Mg ALLOY STRUCTURES, CUBIC S-N CURVE

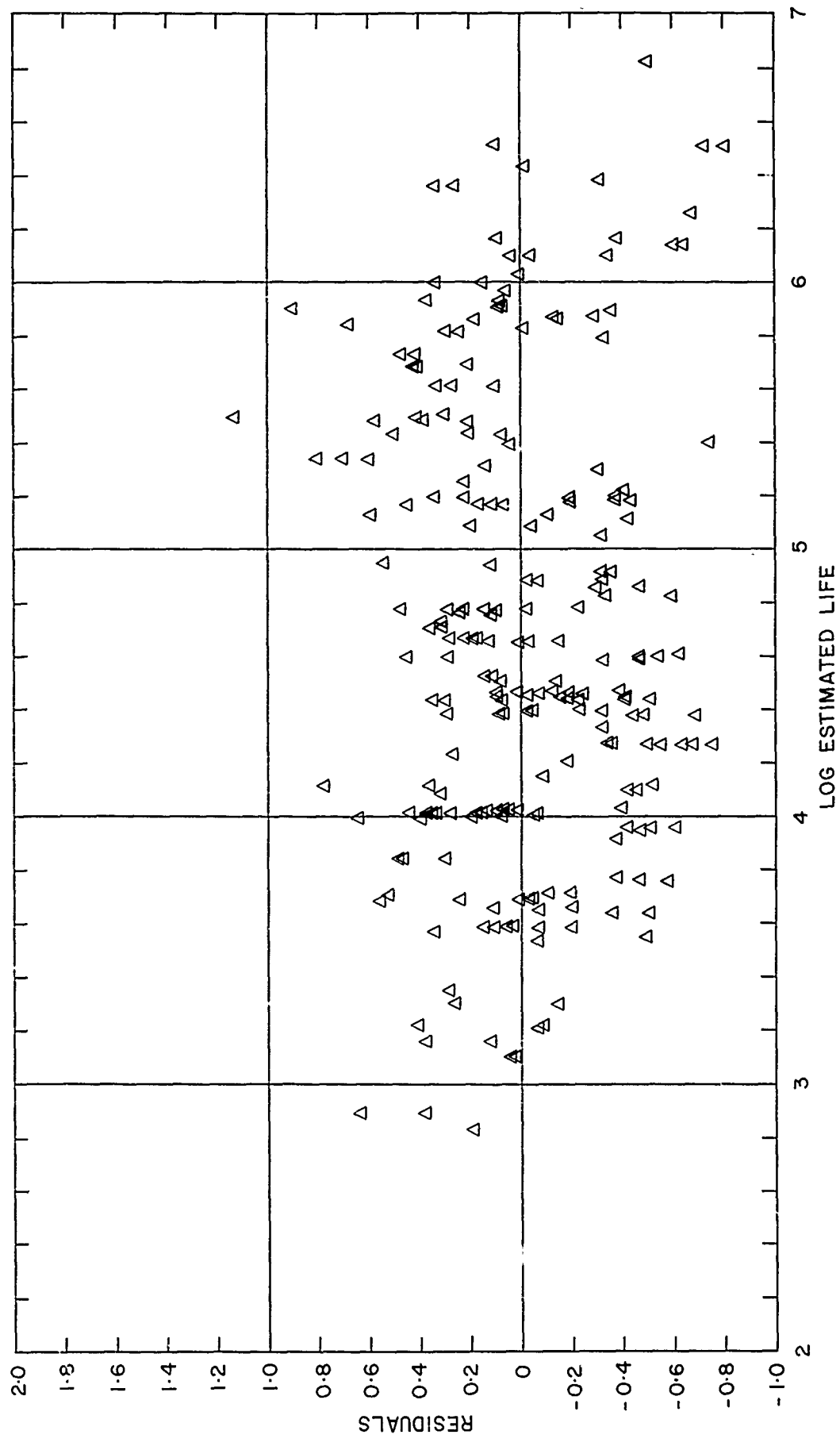


FIG. 14: RESIDUALS VS. ESTIMATED LIFE FOR S-N CURVE NO. 1 (ALL ALLOYS)

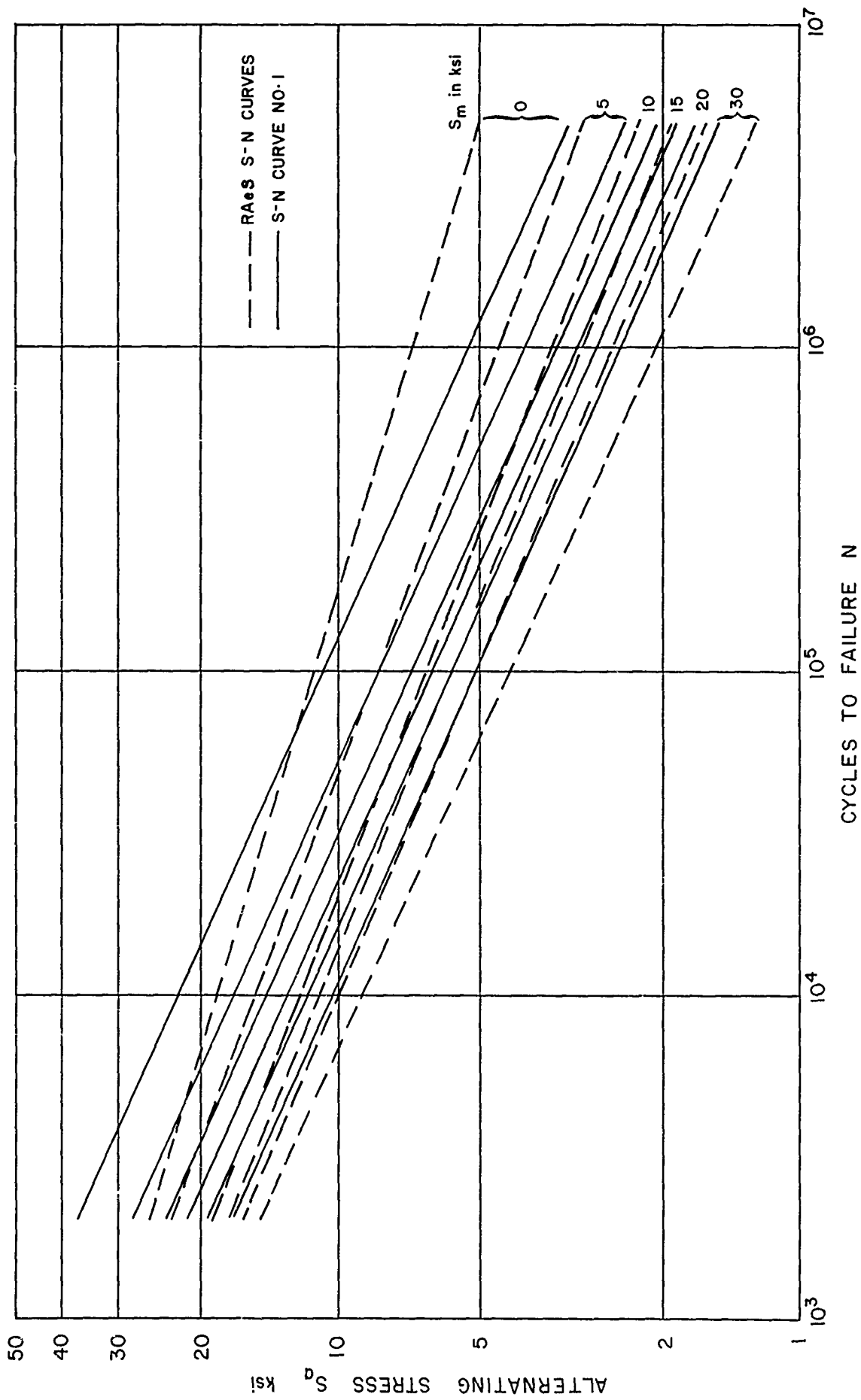


FIG. 15: COMPARISON OF RAeS S-N CURVES AND S-N CURVE NO. 1 (Al-Cu-Mg)

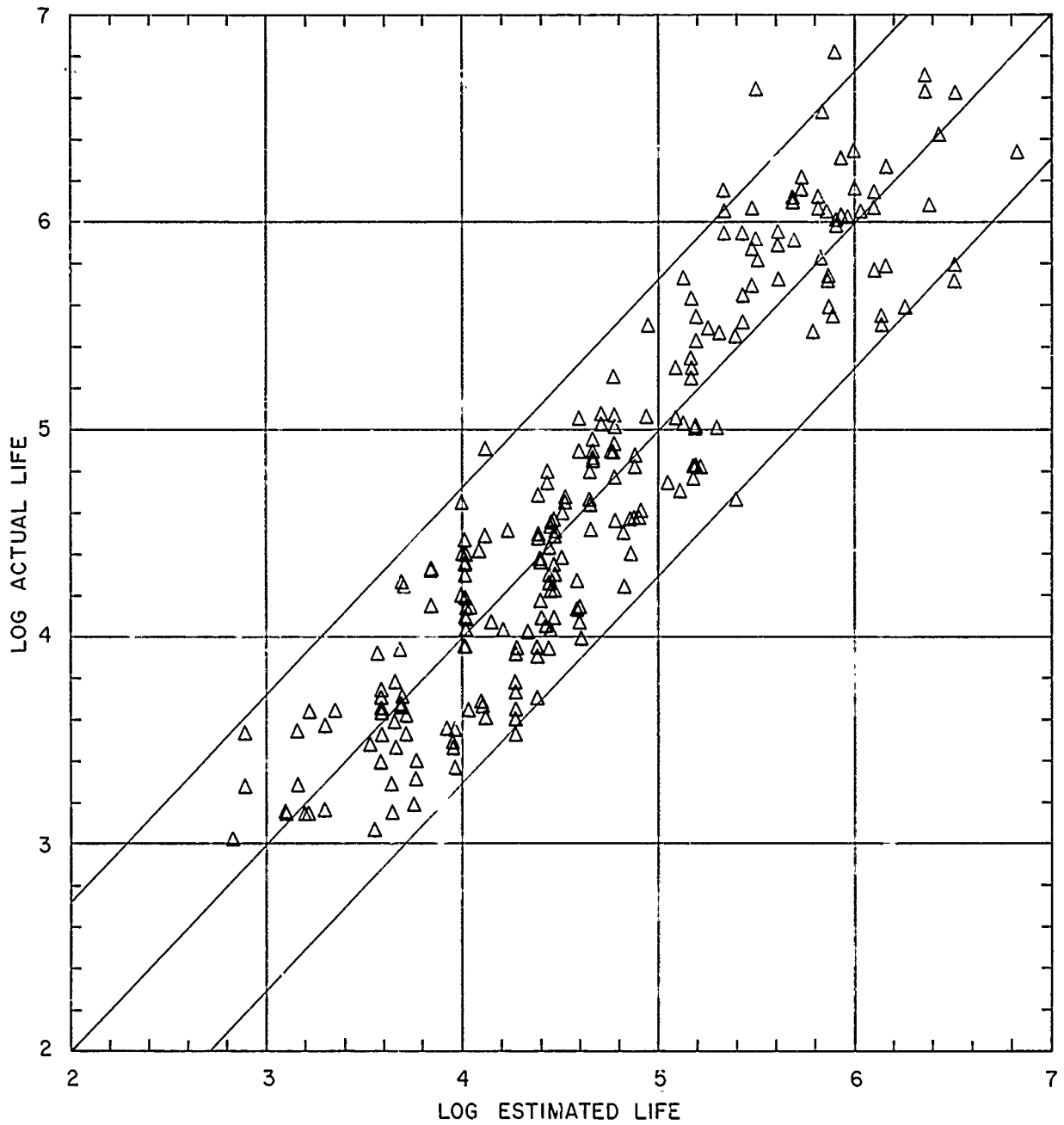


FIG-16: ACTUAL VS. PREDICTED LIVES FOR S-N CURVE NO. 1 (ALL ALLOYS)

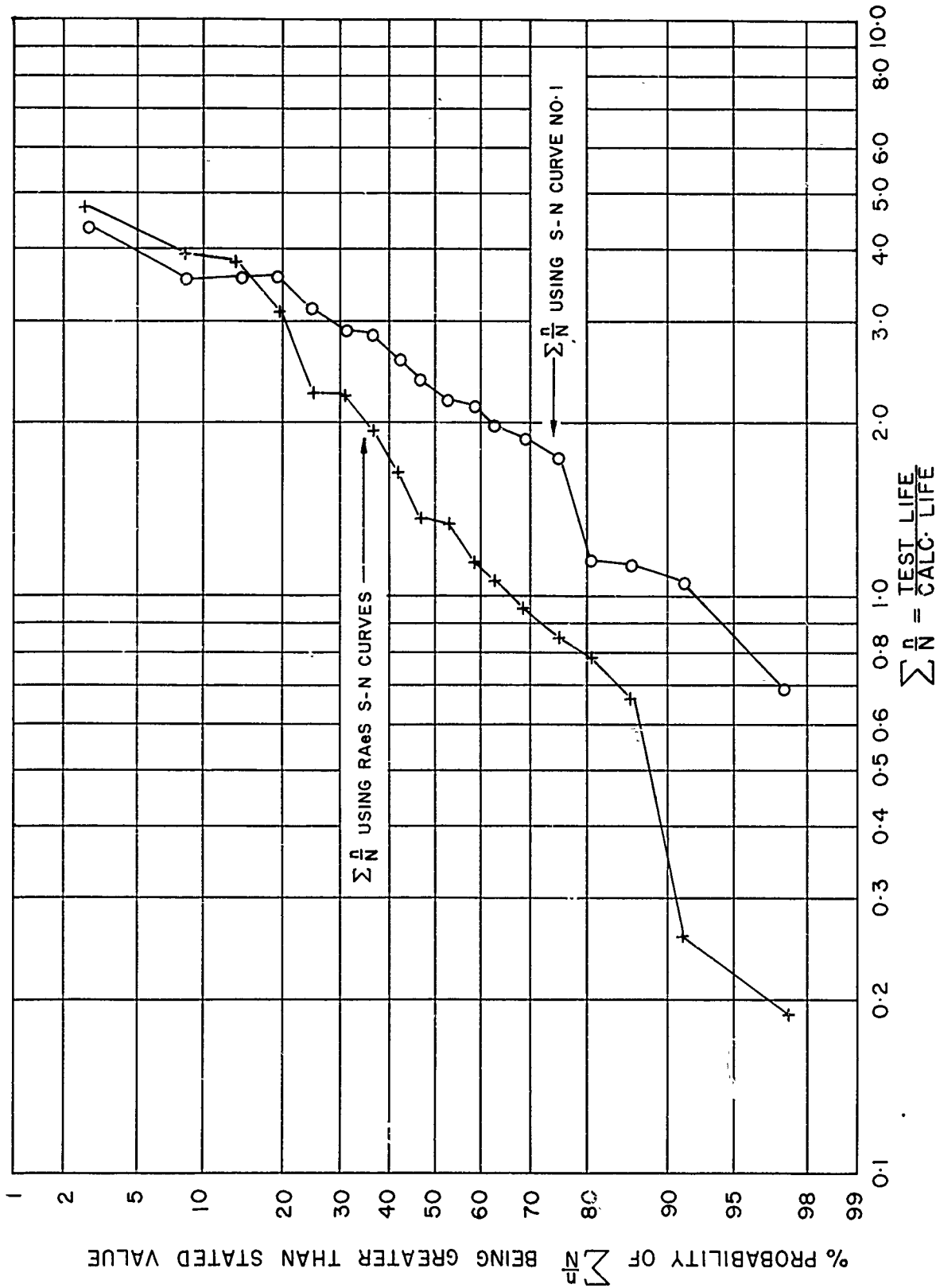


FIG. 17: PROBABILITY OF DAMAGE RATIOS BEING EXCEEDED FOR S-N CURVE NO.1 AND RAeS S-N CURVES

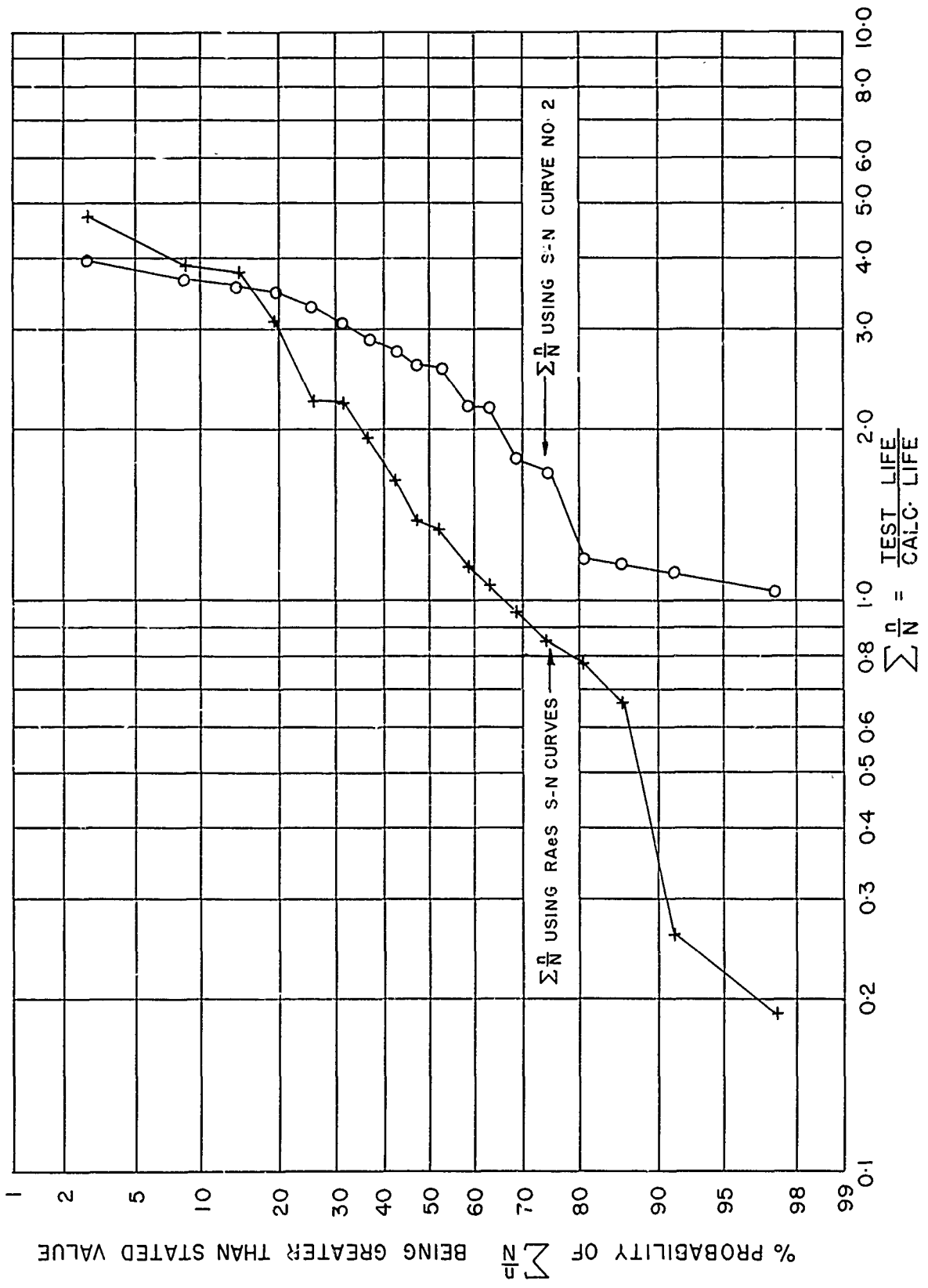


FIG. 18: PROBABILITY OF DAMAGE RATIOS BEING EXCEEDED FOR S-N CURVE NO. 2 AND RAeS S-N CURVES

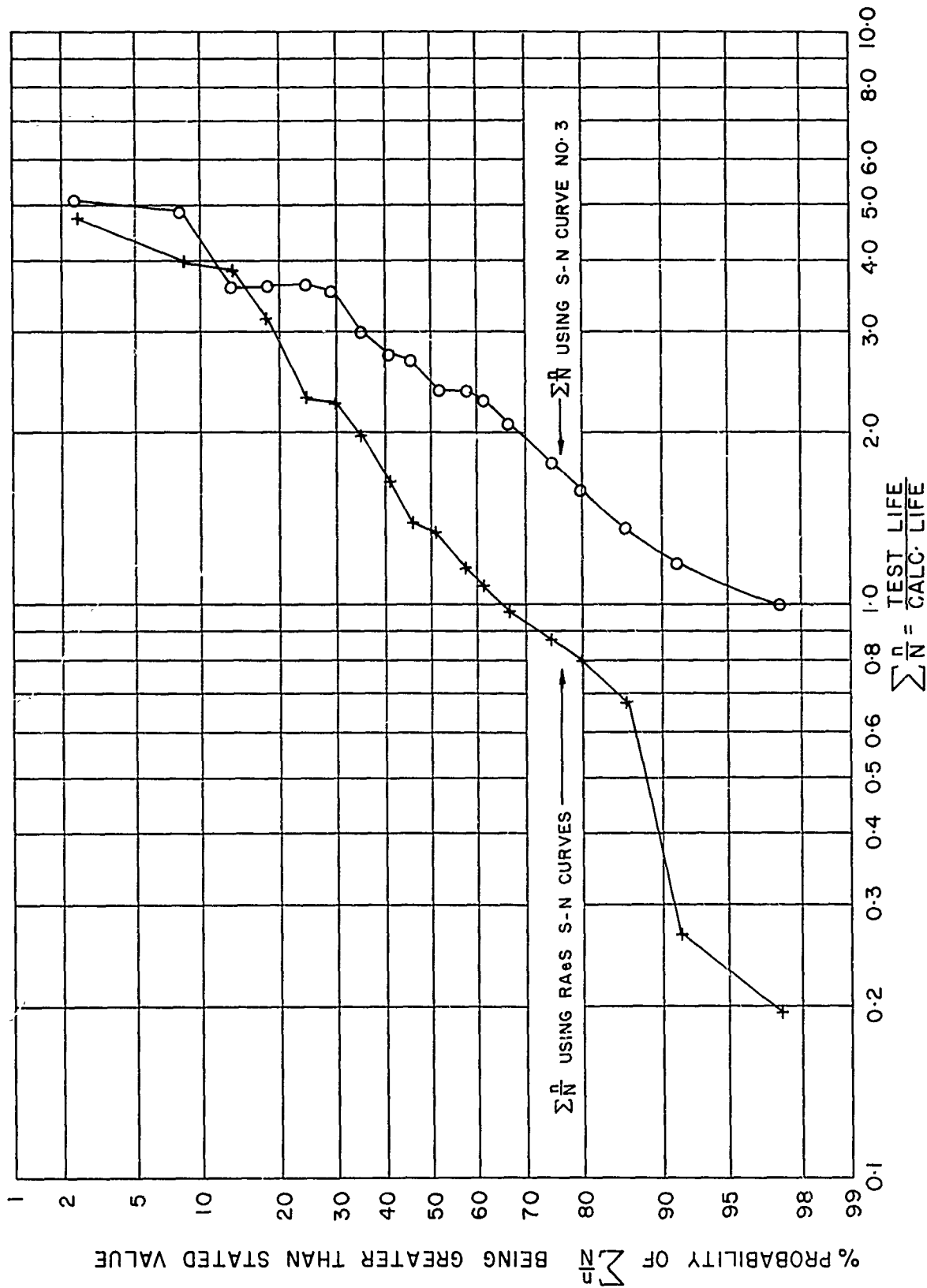


FIG. 19: PROBABILITY OF DAMAGE RATIOS BEING EXCEEDED FOR S-N CURVE NO. 3 AND RAES S-N CURVES

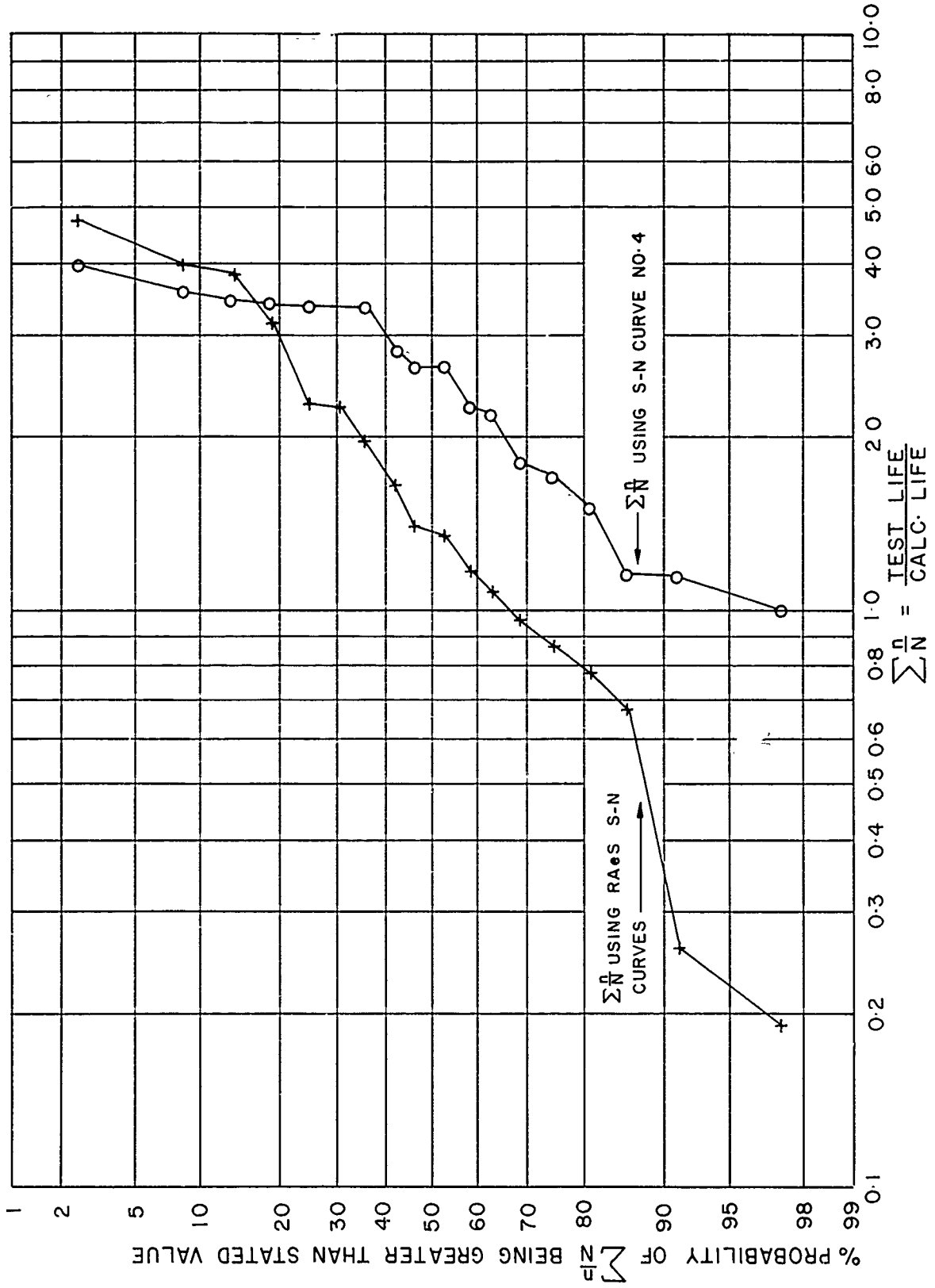


FIG. 20: PROBABILITY OF DAMAGE RATIOS BEING EXCEEDED FOR S-N CURVE NO. 4 AND RAES S-N CURVE

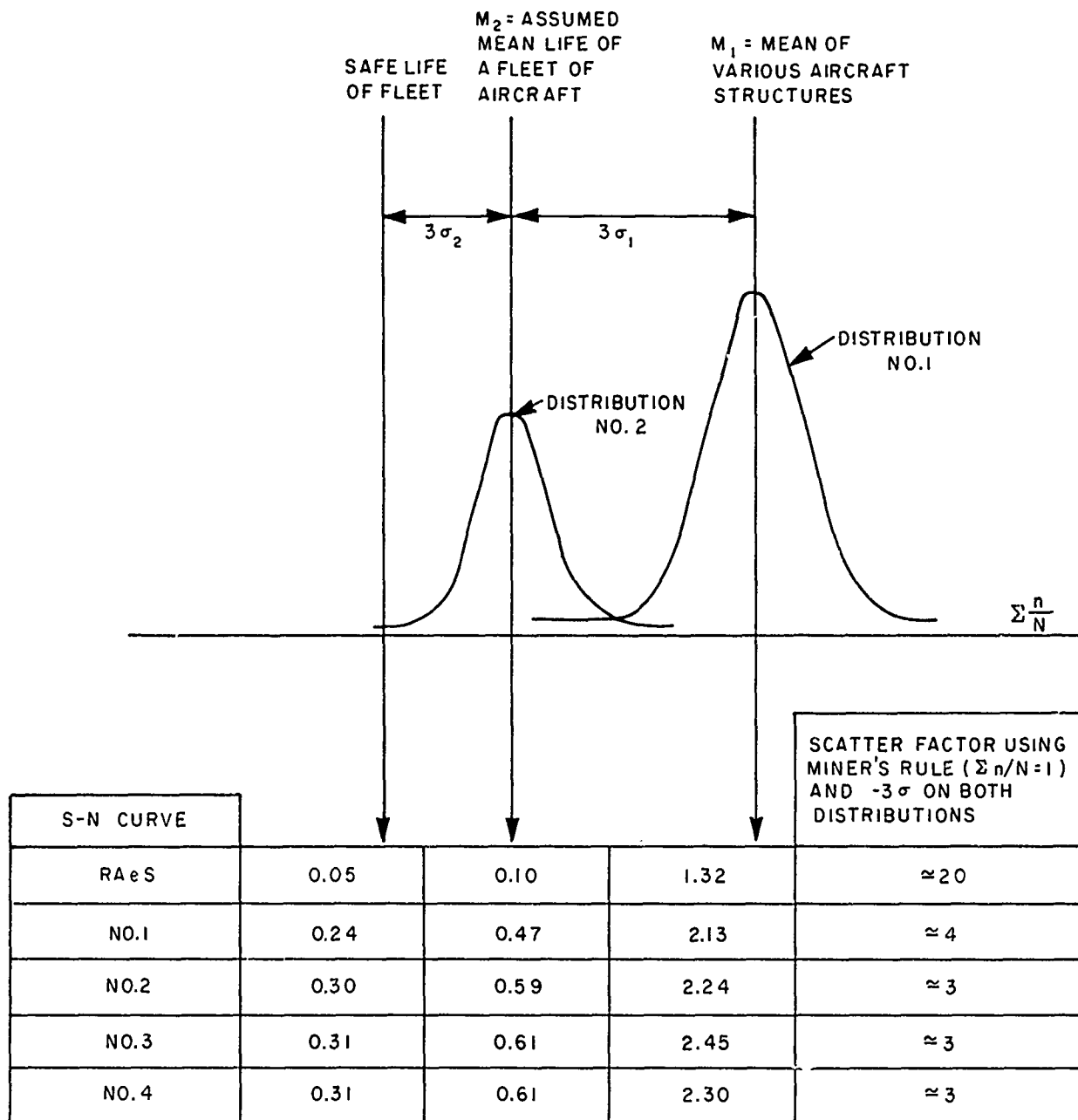


FIG.21: COMPARISON OF  $\sum \frac{n}{N}$  VALUES FOR VARIOUS S-N CURVES AT EQUAL RELIABILITIES

APPENDIX I

METHODS FOR INTERPOLATING BETWEEN THE RAeS S-N CURVES

In general the equation of the curves are given as

$$\log_{10} N = A + B \cdot \log_{10} S_a$$

1. Sewell's Method (Ref. 17)

$$2 \leq S_m < 20 \quad A = 9.45982 - 0.237677 \cdot S_m + 0.0118776 \cdot S_m^2 - 0.00025697 \cdot S_m^3$$

$$B = 3.96687 - 0.021367 \cdot S_m - 0.0004786 \cdot S_m^2 + 0.00000657 \cdot S_m^3$$

2. Douglas' Method (Ref. 18)

$$0 \leq S_m < 2 \quad A = 10.0556 - 0.51285 \cdot S_m$$

$$B = 4.8023 - 0.44000 \cdot S_m$$

$$2 \leq S_m < 15 \quad \text{Sewell's cubic polynomial expressions}$$

$$15 \leq S_m < 20 \quad A = 8.5278 - 0.055198 \cdot S_m$$

$$B = 3.9947 - 0.028920 \cdot S_m$$

$$20 \leq S_m \leq 30 \quad A = 8.3050 - 0.044055 \cdot S_m$$

$$B = 3.9237 - 0.025373 \cdot S_m$$

$S_a, S_m$  in ksi

APPENDIX II

COMPUTER OUTPUT OF TYPICAL LIFE CALCULATION

CF100

DAMAGE IS BASED ON 1000 HOURS. RAES S-N CURVES

ALUMINUM-ZINC-MAGNESIUM ALLOY STRUCTURE

STRESS PER G= 3.500 KSI

INTERVAL	G MEAN	G ALT	S MEAN KSI	S ALT KSI	CYCLES	N	DAMAGE	CUMULATIVE DAMAGE
1	1.625	0.625	5.688	2.188	0.408200D 04	0.138868D 08	0.293948D-03	0.293948D-03
2	1.875	0.875	6.563	3.063	0.202800D 04	0.307637D 07	0.659219D-03	0.953167D-03
3	2.125	1.125	7.438	3.938	0.140800D 04	0.979443D 06	0.143755D-02	0.239072D-02
4	2.375	1.375	8.313	4.813	0.856000D 03	0.390445D 06	0.219237D-02	0.458309D-02
5	2.625	1.625	9.188	5.688	0.454000D 03	0.181820D 06	0.249697D-02	0.708006D-02
6	2.875	1.875	10.063	6.563	0.176000D 03	0.949779D 05	0.185306D-02	0.893312D-02
7	3.125	2.125	10.938	7.438	0.600000D 02	0.542151D 05	0.110670D-02	0.100398D-01
8	3.375	2.375	11.813	8.313	0.240000D 02	0.332042D 05	0.722799D-03	0.107626D-01

TOTAL DAMAGE= 0.107626D-01      LIFE= 0.929142D 02      BLOCKS